



**Politecnico  
di Torino**

**Politecnico di Torino**

Mechanical Engineering  
Master's Degree

Academic Year 2023/2024  
Graduation Section December 2024

**Simulation of Hydromechanical Transmission**

**Relatori**

Massimo Rundo  
Roberto Finesso

**Candidato**

Stephanie Carvalho dos Santos

## Summary

This thesis explores the design and performance of hydromechanical transmissions, focusing on both input-coupled (IC) and output-coupled (OC) configurations. The study begins with an overview of hydromechanical transmission components, including hydrostatic systems and planetary gear trains, and examines how these elements interact in the different transmission configurations.

Using Simcenter Amesim, simulations were performed to analyze the system's behavior under various operating conditions, starting with a constant load scenario. For both IC and OC configurations, results highlighted unique power and torque distribution patterns between hydrostatic and mechanical paths, reflecting each configuration's approach to handling power demands. Further simulations incorporated vehicle dynamics, evaluating speed response, output torque, and power ratios in both configurations. Afterward, a Proportional-Integral-Derivative (PID) control simulation was used to optimize speed tracking, demonstrating how each configuration responds to control adjustments. Finally, simulations examined the system on inclined surfaces and analyzed the effect of changing parameters on the IC configuration, such as varying transmission ratios.

# Contents

Summary .....	2
Contents .....	3
List of Tables.....	5
List of Figures .....	6
Chapter 1. Introduction.....	9
Chapter 2. Introductory Concepts.....	12
2.1. Main Components of Hydromechanical Transmission.....	12
2.1.1. Hydrostatic Transmissions .....	12
2.1.2. Planetary Gear Train .....	13
2.2. Hydromechanical Transmission.....	15
2.2.1. Input Coupled (IC).....	16
2.2.2. Output Coupled (OC).....	19
2.2.3. Compound Coupled .....	22
Chapter 3. Simulation Model.....	25
3.1. Hydrostatic Transmission Model .....	25
3.1.1. Planetary Gear Train .....	26
3.1.2. Gear Models.....	26
3.1.3. Vehicle Model .....	28
3.1.4. Control .....	29
Chapter 4. Constant Load Simulations .....	31
4.1. Simulation Setup.....	31
4.2. Results.....	33
Chapter 5. Vehicle Model Simulations .....	35
5.1. Simulation Setup.....	35
5.2. Results.....	37
5.2.1. Vehicle Speed Response .....	37
5.2.2. Output Torque .....	37
5.2.3. Power Ratio.....	38
Chapter 6. PID Control Simulation .....	40
6.1. Simulation Setup.....	40
6.2. Results.....	40

6.2.1.	Vehicle Speed Response and Displacement Control .....	40
6.2.2.	Output torque .....	41
6.2.3.	Power ratio .....	42
Chapter 7.	Vehicle on Slopes .....	44
7.1.	Simulation Setup .....	44
7.1.1.	Positive Slope.....	44
7.1.2.	Negative Slope .....	44
7.2.	Output Couple Results .....	45
7.2.1.	Low speed .....	45
7.2.2.	High speed .....	47
7.3.	Input Coupled Results.....	49
7.3.1.	Low Speed .....	50
7.3.2.	High Speed.....	51
Chapter 8.	Analysis of Input Coupled Configuration.....	54
8.1.	Effect of Primary Unit Displacement .....	55
8.2.	Effect of Secondary Unit Displacement .....	58
8.3.	Effect of Transmission Ratio Between Prime Mover and Primary Hydraulic Unit ( <b><math>i_1</math></b> ) 61	
8.4.	Effect of Transmission Ratio Between HU and Planetary Gear ( <b><math>i_2</math></b> ).....	64
8.5.	Effect of Planetary Gear Transmission Ratio ( <b><math>\tau_0</math></b> ) .....	67
Chapter 9.	Conclusion .....	70
	Bibliography .....	71
	Appendix.....	72

## List of Tables

Table 1: Vehicle characteristics.....	28
Table 2: Aerodynamics and rolling parameters .....	29
Table 3: Constant load simulation parameters .....	31
Table 4: Vehicle model simulation parameters .....	36
Table 5: Reference values for a batch run.....	54

## List of Figures

Figure 1 - Characteristics of the ICE and vehicle resistance curve. [8].....	9
Figure 2 - Comparison between torque characteristics and ideal traction curve. [6] .....	10
Figure 3 – Torque characteristics when a four-gear transmission is used. [6].....	10
Figure 4 - Torque characteristics of a hydrostatic transmission [8].....	11
Figure 5 - Simplified scheme for hydrostatic transmissions [8].....	12
Figure 6 - Detailed scheme of a hydrostatic transmission [8] .....	13
Figure 7 - Representation of the PGT [8] .....	13
Figure 8 - Power split on the PGT [8].....	14
Figure 9 - PGT power mode [8].....	15
Figure 10: Configuration of shaft connection to the PGT .....	16
Figure 11: Input coupled scheme [1] .....	16
Figure 12: vehicle's speed control through $\alpha$ in IC.....	17
Figure 13: Graphical representation of the PGT's speeds and power flow of the IC with the vehicle at zero speed .....	18
Figure 14: Graphical representation of the PGT's speeds and power flow of the IC with the vehicle at a speed lower than the lockup point .....	18
Figure 15: Graphical representation of the PGT's speeds and power flow of the IC at the lockup point .....	19
Figure 16: Graphical representation of the PGT's speeds and power flow of the IC with the vehicle at a speed greater than the lockup point .....	19
Figure 17: Output coupled Scheme a) Hydraulic differential; b) Planetary gear train [1] .....	20
Figure 18: Control of vehicle's speed through $\alpha$ in OC.....	20
Figure 19: Graphical representation of the PGT's speeds and power flow of the OC with the vehicle at zero speed.....	21
Figure 20: Graphical representation of the PGT's speeds and power flow of the OC with the vehicle at a speed lower than the lockup point .....	21
Figure 21: Graphical representation of the PGT's speeds and power flow of the OC with the vehicle at the lockup point .....	22
Figure 22: Graphical representation of the PGT's speeds and power flow of the OC with the vehicle at a speed greater than the lockup point .....	22
Figure 23: Compound coupled scheme. [1].....	22
Figure 24: Power flow of the CC with the vehicle at a speed smaller than the first lockup point .....	23
Figure 25: Power flow of the CC with the vehicle at a speed between the two lockup points	23
Figure 26: Power flow of the CC with the vehicle at a speed greater than the second lockup point .....	23
Figure 27: Compound coupled architecture hydraulic units operation [3] .....	24
Figure 28: Simcenter Amesim model of the hydrostatic transmission .....	25
Figure 29: Simcenter Amesim's planetary geartrain model .....	26
Figure 30: Simcenter Amesim's 3-port gear model .....	27
Figure 31: Simcenter Amesim's 4-port gear model .....	27

Figure 32: Simcenter Amesim's Reducer model .....	28
Figure 33: Simcenter Amesim's longitudinal vehicle model .....	29
Figure 34: Model of the PID control.....	30
Figure 35: OC Sequential displacement control .....	30
Figure 36: IC Sequential displacement control.....	30
Figure 37: OC constant load simulation model schematics.....	31
Figure 38: IC constant load simulation model schematics .....	32
Figure 39: OC displacement control .....	32
Figure 40: IC displacement control.....	33
Figure 41: OC constant load power ratio .....	33
Figure 42: IC constant load power ratio .....	34
Figure 43: IC and OC transmission torque .....	34
Figure 44: Displacement control.....	35
Figure 45: OC vehicle model simulation schematics .....	36
Figure 46: IC vehicle model simulation schematics .....	36
Figure 47: Speed profiles of vehicle model simulation .....	37
Figure 48: Torque profile at the transmission's output shaft .....	38
Figure 49: OC and IC torque distribution .....	38
Figure 50: OC and IC power ratio .....	39
Figure 51: Requested speed profile.....	40
Figure 52: Vehicle's linear velocity response .....	41
Figure 53: Hydraulic units' displacement .....	41
Figure 54: Output shaft's torque.....	42
Figure 55: OC and IC torque distribution .....	42
Figure 56: OC and IC power ratio .....	43
Figure 57: OC displacement control on slope.....	45
Figure 58: IC displacement control on slope .....	45
Figure 59: OC low speed _ vehicle speed on a slope .....	46
Figure 60: OC low speed _ flow rate through the relief valve.....	46
Figure 61: OC low speed _ pressure drop between high and low-pressure lines .....	47
Figure 62: OC low speed _ Power Ratio .....	47
Figure 63: OC high speed _ pressure at high-pressure line .....	48
Figure 64: OC high-speed _ flow rate through the relief valve .....	48
Figure 65: OC high-speed _ vehicle speed on a slope .....	49
Figure 66: OC high-speed _ Power Ratio .....	49
Figure 67: IC low-speed _ vehicle speed on a slope.....	50
Figure 68: IC low-speed _ flow rate through the relief valve.....	50
Figure 69: IC low speed _ pressure drop between high and low-pressure lines.....	51
Figure 70: IC low speed _ Power Ratio .....	51
Figure 71: IC high speed _ pressure at high pressure-line.....	52
Figure 72: IC high speed _ flow rate through the relief valve .....	52
Figure 73: IC high speed _ vehicle speed on a slope .....	53
Figure 74: IC high speed _ Power Ratio .....	53

Figure 75: Requested speed profile.....	54
Figure 76: Displacement control.....	55
Figure 77: Vehicle speed.....	56
Figure 78: Pressure drop between high and low-pressure lines.....	56
Figure 79: Flow rate through the relief valve .....	57
Figure 80: Power ratio .....	57
Figure 81: Scenario 2 - Vehicle speed.....	58
Figure 82: Displacement control.....	59
Figure 83: Vehicle speed.....	59
Figure 84: Flow rate through the relief valve .....	60
Figure 85: Pressure drop between high and low-pressure lines.....	60
Figure 86: Power ratio .....	61
Figure 87: Scenario 2 - Vehicle speed.....	61
Figure 88: Displacement control.....	62
Figure 89: Vehicle speed.....	62
Figure 90: Pressure drop between high and low-pressure lines.....	63
Figure 91: Flow rate through the relief valve .....	63
Figure 92: Power ratio .....	64
Figure 93: Displacement control.....	65
Figure 94: Vehicle speed.....	65
Figure 95: Pressure drop between high and low-pressure lines.....	66
Figure 96: Flow rate through the relief valve .....	66
Figure 97: Power ratio .....	67
Figure 98: Scenario 2 - Vehicle speed.....	67
Figure 99: Displacement control.....	68
Figure 100: Vehicle speed.....	68
Figure 101: Pressure drop between high and low-pressure lines.....	69
Figure 102: Flow rate through the relief valve .....	69
Figure 103: Power ratio .....	69

# Chapter 1. Introduction

In recent years, the automotive industry has been under intense pressure to improve vehicle efficiency, reduce emissions, and optimize performance. These demands have led to the evolution of innovative drivetrain technologies, including hybrid systems, electric drivetrains, and advanced mechanical transmissions. Among these, hydromechanical transmissions (HMTs) have emerged as a compelling solution due to their ability to combine the efficiency of mechanical transmissions with the flexibility of hydrostatic systems.

HMTs provide a unique approach by distributing power through both mechanical and hydraulic paths, allowing for smoother power delivery, better efficiency, and enhanced vehicle performance across a wide range of operating conditions. This dual-path mechanism has garnered significant interest, particularly in heavy machinery, agriculture, and on-road vehicles, where performance and fuel economy are critical.

The transmission is a key component in every vehicle, playing a crucial role in transforming the available power supplied by the engine to meet the speed and torque requirements of the vehicle. In Figure 1, it is possible to observe on the left side the typical torque and power characteristics for an internal combustion engine (ICE) at full throttle and on the right side the ideal traction curve at constant power and the typical vehicle resistance curve, which is a result of the vehicle mass, the ground profile, the rolling friction, and the aerodynamics resistance.

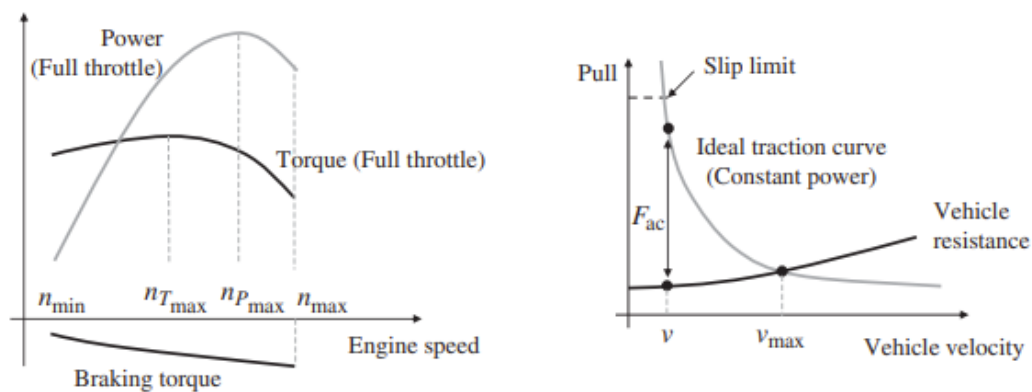


Figure 1 - Characteristics of the ICE and vehicle resistance curve. [8]

In Figure 2 the torque characteristics of the ICE and the ideal traction curve are drawn in the same chart, helping to visualize that connecting the wheels directly to the ICE would be impossible to perform the whole mission and the shaded area would not be achieved.

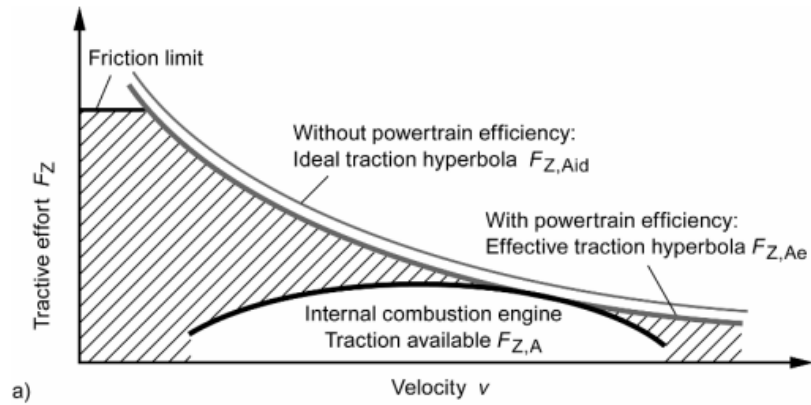


Figure 2 - Comparison between torque characteristics and ideal traction curve. [6]

The transmission is the part of the power train that approximates the engine’s torque characteristics to the traction hyperbola as shown in Figure 3, when a four-gear mechanical transmission is used.

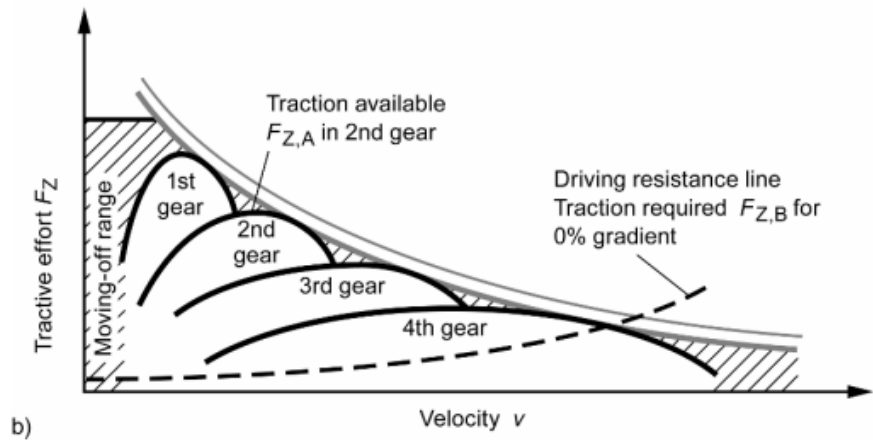


Figure 3 – Torque characteristics when a four-gear transmission is used. [6]

As can be observed in Figure 4, hydrostatic transmission has torque characteristics more similar to the ideal traction hyperbola, which means that the use of hydrostatic transmission allows a greater range of use, and it can operate in scenarios not achievable with the mechanical transmission. However, hydrostatic transmissions have lower efficiency when compared to mechanical transmission. Hydro-mechanical transmission (HMT) allows a balance between hydrostatic transmission’s flexibility and mechanical transmission’s high efficiency.

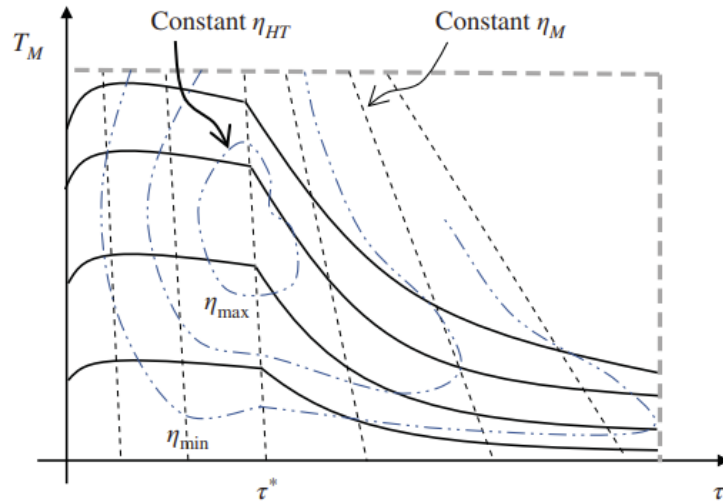


Figure 4 - Torque characteristics of a hydrostatic transmission [8]

The primary goal of this thesis is to explore the performance characteristics of different HMT configurations, with a specific focus on:

1. **Understanding power distribution and efficiency:** Analyze how power is split between the mechanical and hydraulic paths in each configuration.
2. **Evaluating control strategies:** Investigate how vehicle speed and torque are controlled through hydraulic unit displacements.
3. **Assessing different scenarios:** Simulate various driving conditions, including constant acceleration, slope operations, and PID-controlled speed profiles.

The study of hydromechanical transmissions is pivotal for advancing modern vehicle technology. By examining their configurations, control strategies, and performance under various conditions, this thesis aims to provide a foundation for future research and development in the field.

## Chapter 2. Introductory Concepts

### 2.1. Main Components of Hydromechanical Transmission

#### 2.1.1. Hydrostatic Transmissions

Classified as a continuously variable transmission, according to ISO standards 5598 and 4391, a hydrostatic transmission is a “combination of one or more hydraulic pumps and motors forming a unit designed to obtain a variation of speed or torque.” It can be used either in an open or closed circuit, as illustrated in the simplified scheme in Figure 5. For the present thesis, only the closed configuration is worth discussing.

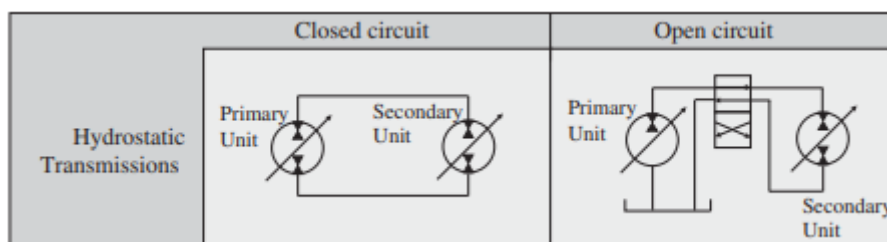


Figure 5 - Simplified scheme for hydrostatic transmissions [8]

A hydrostatic transmission is composed of two hydraulic units (HU), that can operate either as a pump or as a motor. Usually, the unit connected to the prime mover is referred to as the primary unit, and the one connected to the load is referred to as the secondary unit. Even though both units can operate as a pump or as a motor, it is common to call the primary unit a “pump” and the secondary unit a “motor”, when talking about hydrostatic transmission. Both units can be fixed displacement units or variable displacement units, but to be considered a continuously variable transmission, at least one of the units must be a variable displacement unit.

To ensure proper internal lubrication flow, both units must have external drains that are directly connected to the tank. The fluid lost through the drains can be detrimental to the system, as it reduces the pressure in the low-pressure line and the pump would operate under severe cavitation. To avoid the early failure of the transmission, the hydrostatic transmission must be equipped with a charging circuit, which assures a minimum pressure at the low-pressure line, composed of:

- Charging pump;
- Relief valve;
- Two check valves.

Furthermore, it is also necessary to add two relief valves to limit the maximum pressure in the high-pressure line, referred to as cross-port relief valves, and a flushing circuit, which allows the proper cooling of the transmission, composed of a relief valve and a 3/3 directional control valve. A schematic of all the elements mentioned is illustrated in Figure 6.

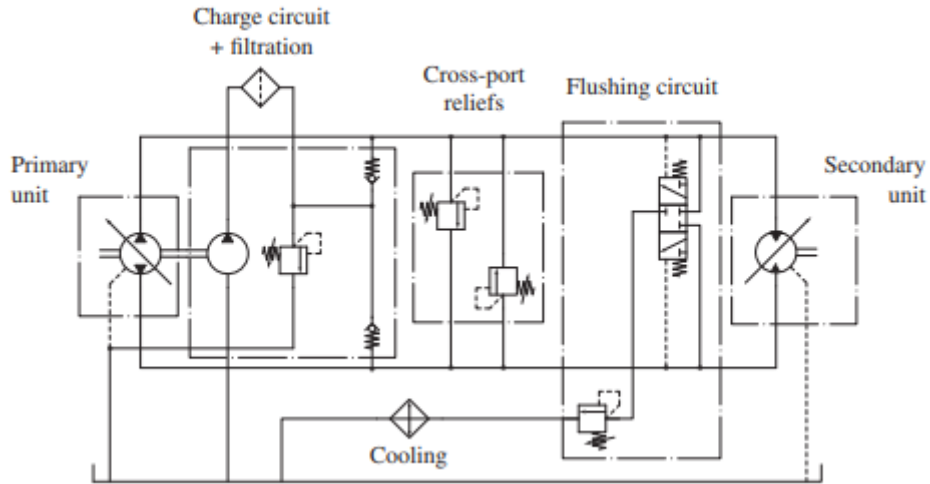


Figure 6 - Detailed scheme of a hydrostatic transmission [8]

In hydrostatic transmission, there is a flow coupling of the hydraulic units, which means that the flow delivered by the primary unit is received by the secondary unit. [9] See eq. (1):

$$\alpha_I \cdot V_I \cdot \omega_I \cdot \eta_{V_I} = \frac{\alpha_{II} \cdot V_{II} \cdot \omega_{II}}{\eta_{V_{II}}} \quad (1)$$

In which  $\alpha$  is the ratio between the current and maximum displacement of the hydraulic unit,  $V$  is the maximum displacement,  $\omega$  is the angular velocity of the unit, and  $\eta_v$  is the volumetric efficiency. The subscript  $I$  refers to the primary unit while the subscript  $II$  refers to the secondary unit.

### 2.1.2. Planetary Gear Train

The planetary gear train (PGT) is the mechanical device that allows the mechanical power to be either split or combined between the shafts connected to it. Typically, a PGT is composed of a sun gear, a ring gear, planet gears, and the carrier, which is a rotating element that supports the sun and the planet gears. In Figure 7 a drawing of the elements (right side) and the symbolic representation of the PGT (left side) is shown.

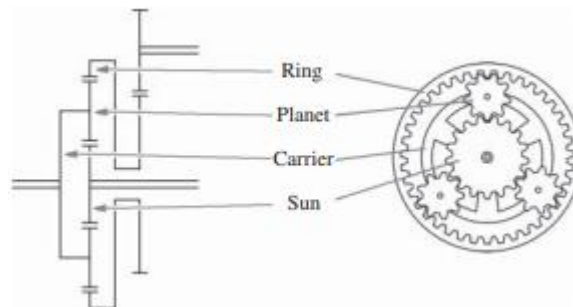


Figure 7 - Representation of the PGT [8]

The Willis equation gives the relationship between the rotational speed of the elements as shown in eq. (2):

$$\omega_S - \tau_0 \omega_R - (1 - \tau_0) \omega_C = 0 \quad (2)$$

Where:

- $\omega_S$  is the angular velocity of the sun gear
- $\omega_R$  is the angular velocity of the ring gear
- $\omega_C$  is the angular velocity of the carrier
- $\tau_0$  is the ratio between the number of teeth of the ring gear ( $Z_R$ ) and the number of teeth of the sun gear ( $Z_S$ ).

$$\tau_0 = -\frac{Z_R}{Z_S} \quad (3)$$

From the torque balance on the PTG, it is possible to obtain the relation in eq. 4.

$$\begin{cases} T_C = (\tau_0 - 1)T_S \\ T_R = -\tau_0 T_S \end{cases} \quad (4)$$

Where:

- $T_C$  is the torque of the carrier
- $T_S$  is the torque of the sun
- $T_R$  is the torque of the ring

The properties of variable speed ratios and fixed torque ratios allow the PGT to split the power between the three gears. The power split obtained by the PTG is schematized in Figure 8.

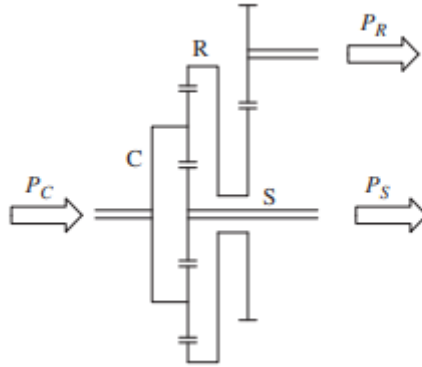


Figure 8 - Power split on the PGT [8]

From eqs. (2) and (4), and considering that ideally  $P_S + P_R + P_C = 0$ , the following power relationship can be derived:

$$\begin{cases} P_S = \frac{P_C}{\tau_0 \frac{\omega_R}{\omega_S} - 1} \\ P_R = \frac{-\tau_0 P_C}{\tau_0 - \frac{\omega_S}{\omega_R}} \end{cases} \quad (5)$$

It is important to highlight that the power can be either positive or negative, meaning that the PGT can operate as a power split or as a power summation, allowing power recirculation within the transmission, as summarized in Figure 9.

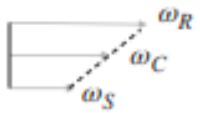
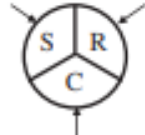
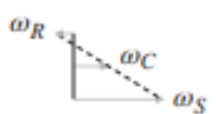
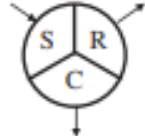
PGT operation	PGT vector representation	Rotational direction	Torque direction	Power direction	Power flow
Summer		+	+	in	
Splitter		-	+	out	

Figure 9 - PGT power mode [8]

The image provides a comparative analysis of the operational modes of a planetary gear train (PGT) in "Summer" and "Splitter" configurations. In the Summer mode, the system combines two input speeds to produce an output speed, while in the Splitter mode, it divides an input speed into two output speeds. The table includes vector representations of the angular velocities of the ring (R), carrier (C), and sun gear (S), illustrating their relationships in each mode. It also details the rotational directions, with positive or negative signs indicating the direction of rotation for each component. Torque direction is similarly represented, showing whether the torque aids or opposes rotation. Additionally, the table outlines the power direction, specifying whether power flows into or out of each component. Power flow diagrams accompany these descriptions, visually depicting the distribution of power among the ring, carrier, and sun gears, with arrows indicating the direction of energy transfer.

## 2.2. Hydromechanical Transmission

According to Kress [5], the hydromechanical transmission can be classified into 3 main categories:

- Input coupled (IC)
- Output coupled (OC)
  - Planetary
  - Hydraulic differential
- Compound coupled

From those, the input and the output coupled are three-shaft systems and the compound coupled is a four-shaft system. In all cases, the shafts are connected either to the output (IC), to the input (OC), or both (compound coupled), through a planetary gear train.

In the three-shaft systems, the shafts can be connected to the planetary gear train in six different configurations as shown in Figure 10. Where "In" stands for the input shaft, "Out" stands for the output shaft, and "HU" stands for the hydraulic unit.

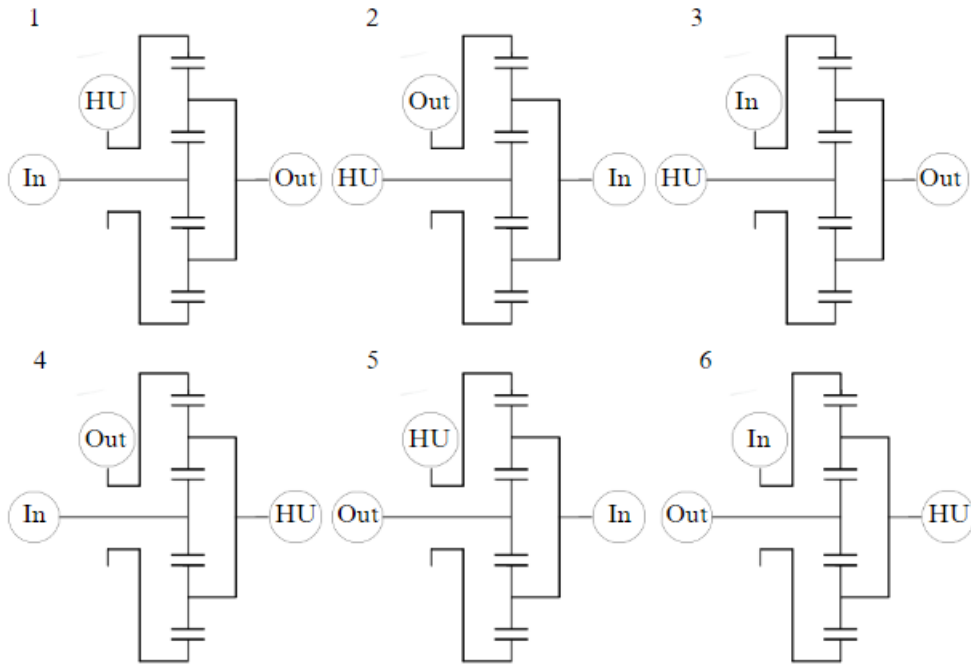


Figure 10: Configuration of shaft connection to the PGT

The Compound-Coupled (CC) configuration is not schematized because it involves a four-shaft system, which makes it impractical to represent due to the sheer number of possible combinations. Unlike the Output-Coupled (OC) and Input-Coupled (IC) configurations, which can be fully described with three shafts (input, output, and hydraulic unit) and six possible configurations, the CC configuration introduces an additional shaft connecting two planetary gear trains. This results in 216 possible combinations of connections, making it highly complex and inefficient to schematize within the scope of the figure.

### 2.2.1. Input Coupled (IC)

This type of transmission can also be identified as “split torque”. One of the hydraulic units (primary unit) is attached to the transmission's input, meaning that the input torque splits into two paths, the mechanical and the hydrostatic. The other hydraulic unit (secondary unit) is connected to the planetary gear train as illustrated in Figure 11.

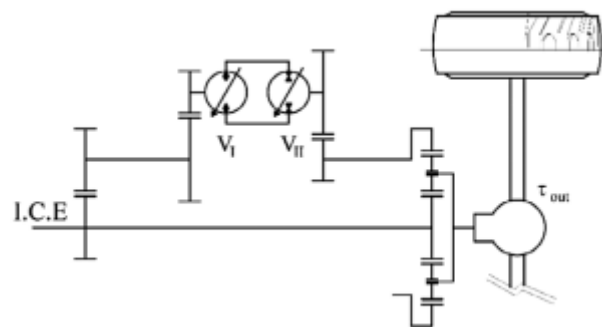


Figure 11: Input coupled scheme [1]

An important concept in hydromechanical transmissions is the lockup point, which is the speed at which power circulation, the flow of energy between the mechanical and hydraulic systems, changes. At this speed, the transmission acts as fully mechanical. In the IC case, the secondary unit stops the “floating” member of the PGT and its speed becomes null.

If the vehicle’s speed is higher than the lockup point’s, the PGT is driven by the secondary unit, which acts as a motor, and the power circulation is said to be “non-regenerative”. If the vehicle speed is lower, the secondary unit, which acts as a pump, is driven by the PGT, and the power adds to the input power, therefore being called “regenerative.”

The vehicle’s speed is controlled by changing the displacement of the hydraulic units. At zero speed, the primary unit’s displacement ( $\alpha_1$ ) is set to a negative value, which depends on the transmission ratio between the primary unit and the prime mover, while the secondary unit’s displacement is set to 100% ( $\alpha_2 = 1$ ). The control is achieved by modifying one displacement at a time, as shown in Figure 12, which illustrates the relationship between  $\alpha$  and the vehicle's speed. The vehicle’s speed increases as the primary unit’s displacement is adjusted, reaching a limit once the primary unit’s maximum displacement is reached. To further increase speed, the secondary unit’s displacement must then be decreased.

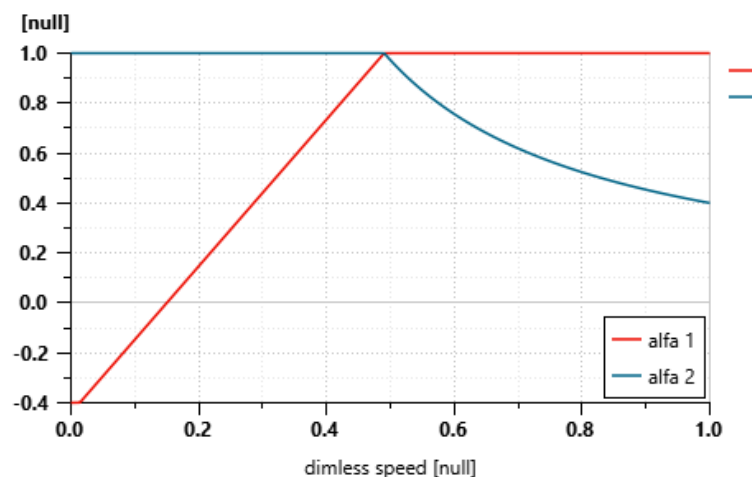


Figure 12: vehicle's speed control through  $\alpha$  in IC

Furthermore, to simplify the operation modes analyses, the engine is considered to be connected to the sun gear, the wheels to the carrier, and the secondary unit to the ring gear (configuration 1 at Figure 10), but as mentioned before, other configurations might be performed. The analysis is then performed as a function of the vehicle speed ( $\omega_c$ ) and divided into four scenarios.

- a) Full power recirculation (regenerative): in this scenario the vehicle is still and therefore  $\omega_c = 0$ . The speeds of the ring ( $\omega_R$ ) and of the sun ( $\omega_S$ ) are related according to the eq. (6) and the power relationship is given by eq. (7), both are respectively shown in Figure 13.

$$\omega_S = \tau_0 \omega_R \quad (6)$$

$$P_R = -P_S \quad (7)$$

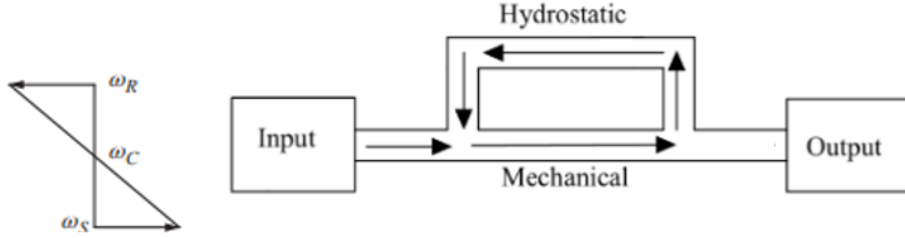


Figure 13: Graphical representation of the PGT's speeds and power flow of the IC with the vehicle at zero speed

- b) Power recirculation (regenerative): in this scenario, the vehicle is at a speed lower than the lockup point's speed. As the vehicle speed increases, the ring speed decreases and can be calculated according to the Whillis Equation (eq. (2)), and its graphical representation can be seen in Figure 14, as well as the power flow in the transmission. The power relationship between the mechanical power ( $P_S$ ) and the hydrostatic power ( $P_R$ ) is given by the eq. (8).

$$P_R = -\omega_R \tau_0 \frac{P_S}{\omega_S} \quad (8)$$

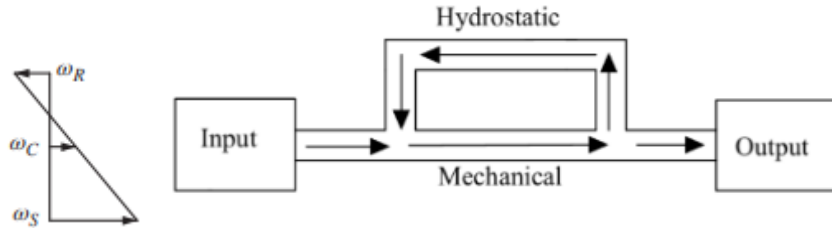


Figure 14: Graphical representation of the PGT's speeds and power flow of the IC with the vehicle at a speed lower than the lockup point

- c) Full mechanical: in this scenario, the power is transmitted fully mechanically, which means that  $P_R = 0$  and  $\omega_R = 0$ . The vehicle reached the so-called lockup point's speed, given by eq. (9). The graphical representation of the speeds and the power flow are illustrated in Figure 15.

$$\omega_C = \frac{\omega_S}{1 - \tau_0} \quad (9)$$

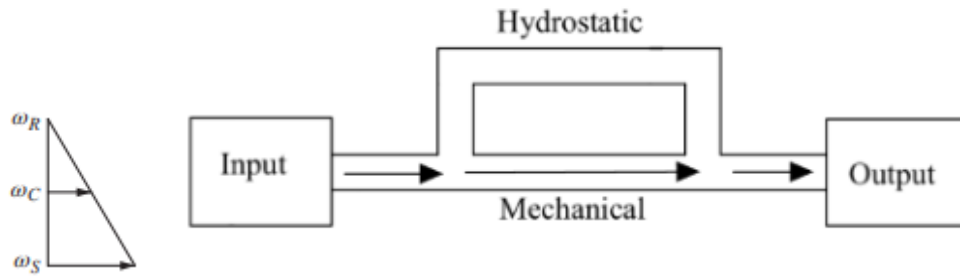


Figure 15: Graphical representation of the PGT's speeds and power flow of the IC at the lockup point

- d) Power additive (non-regenerative): in this scenario, the vehicle speed is beyond the lockup point's speed. Until this point the secondary was acting as a pump and beyond this point it starts to act as a motor due to the change of direction of rotation of the ring gear. The eq. (10) gives the power relationship and the graphical representation of the speeds, and the power flow are illustrated in Figure 16.

$$\begin{cases} \lim_{\omega_R \rightarrow \infty} \frac{P_R}{P_C} = -1 \\ \lim_{\omega_R \rightarrow \infty} \frac{P_S}{P_C} = 0 \end{cases} \quad (10)$$

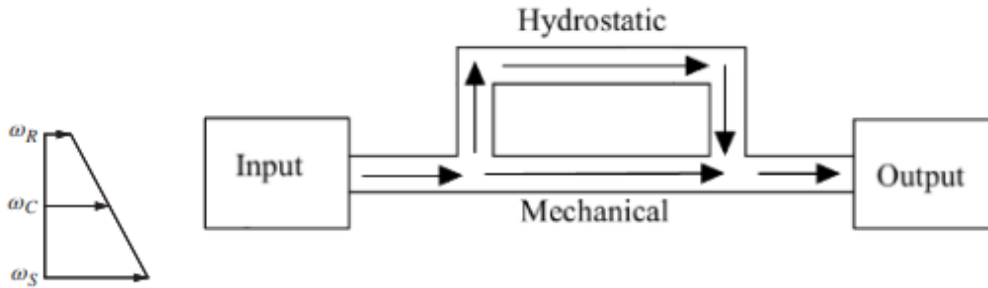


Figure 16: Graphical representation of the PGT's speeds and power flow of the IC with the vehicle at a speed greater than the lockup point

### 2.2.2. Output Coupled (OC)

Also identified as “split speed,” the output coupled is the opposite of the IC. In other words, the prime mover is connected to the primary unit through the PGT, and the secondary unit is connected to the output shaft through regular gears.

It is possible to find two types of it in the literature, the hydraulic differential and the planetary gearset, Figure 17 (a) and (b) respectively. They are analogous in theoretical performance and differ in the hydraulic unit speeds. While the unit speeds in the planetary gearset type are defined through the Willis equation, in the hydraulic differential architecture, the primary unit's effective speed is equal to the output speed ( $\omega_o$ ), and the pumping (or motoring) action is due to the relative motion of the grounded cylinder block and the swashplate. At the secondary unit, the cylinder block rotates at input speed ( $\omega_i$ ) and the swashplate rotates at output speed, thus the speed of the secondary unit is the difference between the input speed and output speed ( $\omega_2 = \omega_i - \omega_o$ ). Furthermore, the efficiency of the hydraulic differential should be slightly

higher than the planetary since the last has mechanical losses associated with the planetary gear.

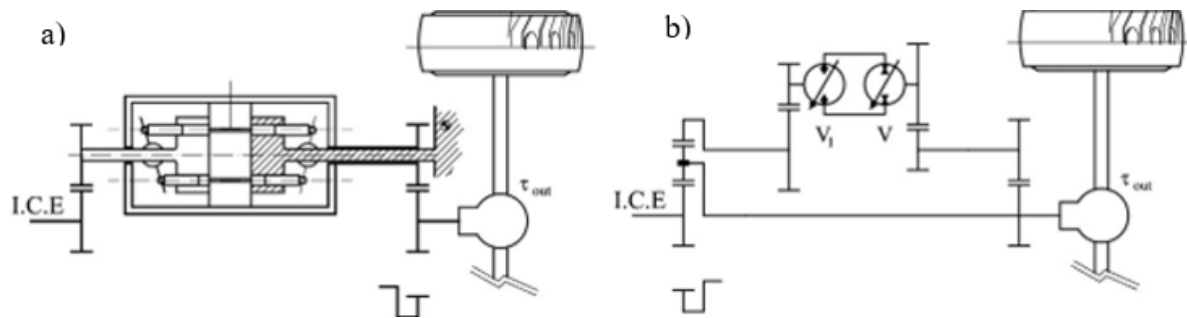


Figure 17: Output coupled Scheme a) Hydraulic differential; b) Planetary gear train [1]

As mentioned before both types have the same theoretical performance, therefore the following analysis is done for the PGT type, considering the engine connected to the carrier, the wheels to the sun gear, and the primary unit to the ring gear (configuration 5 at Figure 10).

In the OC configuration, at the “lockup point,” a small amount of the output power is bled into the hydraulic units and stops the ring gear. Acting in the opposite way as the IC, if the vehicle speed is lower than the lockup point’s speed, the primary unit acts as a pump, and is driven by the PGT, and the power circulation is said to be “non-regenerative.” If the vehicle’s speed is greater, the primary unit acts as a motor and drives the PGT, the power adds to the input power, therefore being called “regenerative.”

Similar to the IC case, the change in the hydraulic units’ displacement controls the vehicle’s speed. When the vehicle is at zero speed the displacement of the primary unit is set to 0% ( $\alpha_1 = 0$ ) and the displacement of the secondary unit is set to 100% ( $\alpha_2 = 1$ ). The control is performed by changing one displacement at a time as shown in Figure 18, the value of  $\alpha$  as a function of the vehicle’s speed. The speed increases to a certain limit while increasing the displacement of the primary unit. After achieving the maximum displacement of it, to further increase the vehicle’s speed, it is necessary to decrease the displacement of the secondary unit.

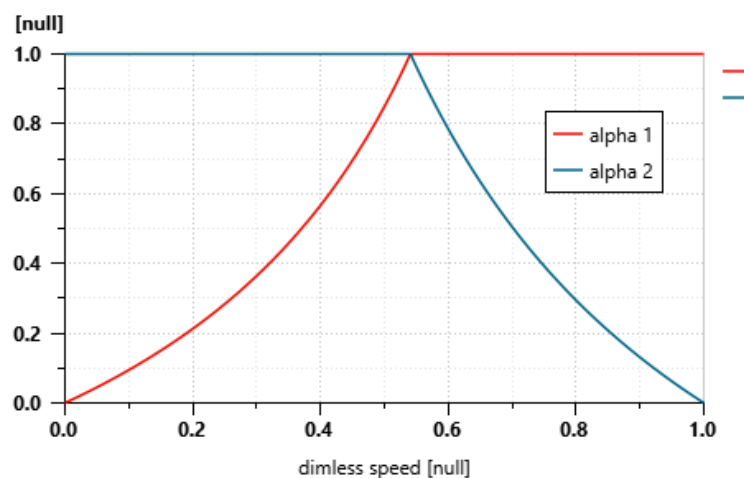


Figure 18: Control of vehicle's speed through  $\alpha$  in OC

- a) Full hydraulic: in this scenario, the vehicle has null speed and therefore  $\omega_S = 0$ . All the power is transmitted to the wheels through the hydrostatic transmission. The speeds of the carrier and the ring can be calculated using eq. (11) and the power relationship with eq. (12), both are respectively shown in Figure 19.

$$\omega_R = \frac{(\tau_0 - 1)\omega_C}{\tau_0} \quad (11)$$

$$P_R = -P_C \quad (12)$$

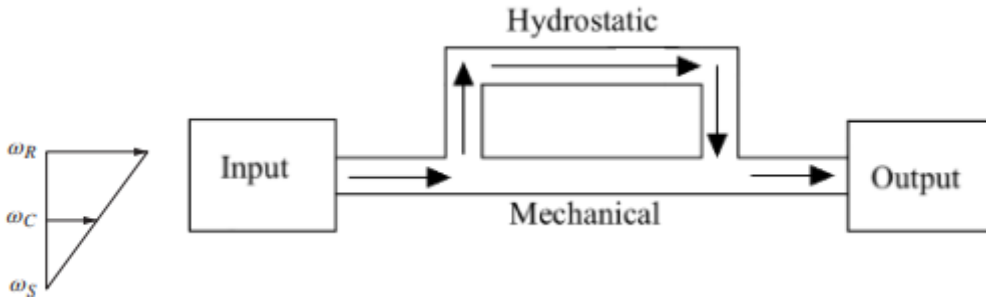


Figure 19: Graphical representation of the PGT's speeds and power flow of the OC with the vehicle at zero speed

- b) Power additive: as the vehicle increases its speed the speed of the hydraulic unit decreases and also the amount of hydraulic power. The speeds can be then calculated through the Willis Equation, eq. (2), and the power ratio is given by the eq. (13). The graphical representation of the speeds as well as the power flow through the transmission can be seen in Figure 20.

$$\begin{cases} \frac{P_C}{P_S} = \frac{(\tau_0 - 1)\omega_C}{\omega_S} \\ \frac{P_R}{P_S} = \frac{(1 - \tau_0)\omega_C - \omega_S}{\omega_S} \end{cases} \quad (13)$$

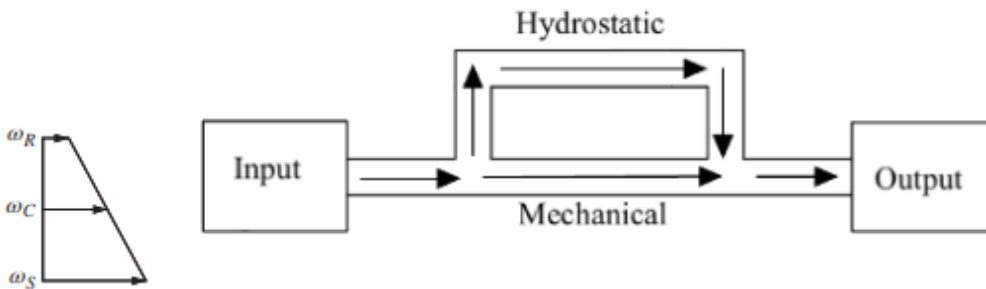


Figure 20: Graphical representation of the PGT's speeds and power flow of the OC with the vehicle at a speed lower than the lockup point

- c) Full mechanical: in this scenario, the lockup point is reached, and the secondary unit has zero displacement. The ring gear's speed is null ( $\omega_R = 0$ ) and consequently, the power through the hydrostatic transmission is null ( $P_R = 0$ ). The graphical representation of the speeds as well as the power flow is shown in Figure 21.

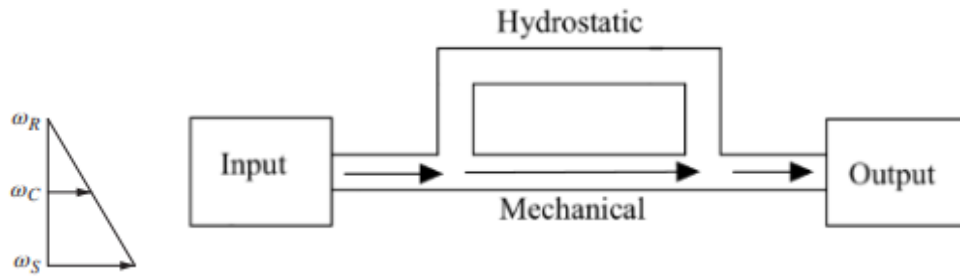


Figure 21: Graphical representation of the PGT's speeds and power flow of the OC with the vehicle at the lockup point

- d) Power recirculation: in this scenario, to further increase the vehicle's speed, the secondary unit inverts its rotation's direction ( $\alpha_2 < 0$ ) and it starts to act as a pump. This mode is characterized by lower efficiencies and should be avoided. The graphical representation of the speeds as well as the power flow is shown in Figure 22.

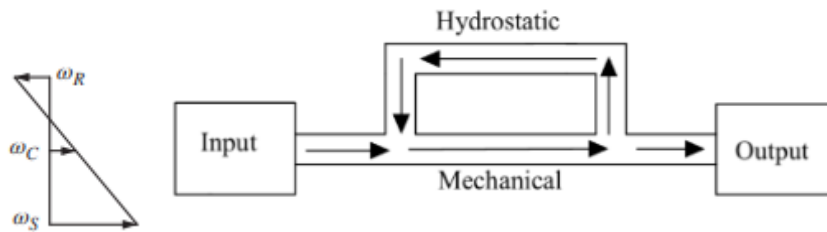


Figure 22: Graphical representation of the PGT's speeds and power flow of the OC with the vehicle at a speed greater than the lockup point

### 2.2.3. Compound Coupled

The compound-coupled hydromechanical transmission (HMT) integrates the characteristics of input-coupled (IC) and output-coupled (OC) configurations, into a four-shaft system with two planetary gear trains, as shown in Figure 23.

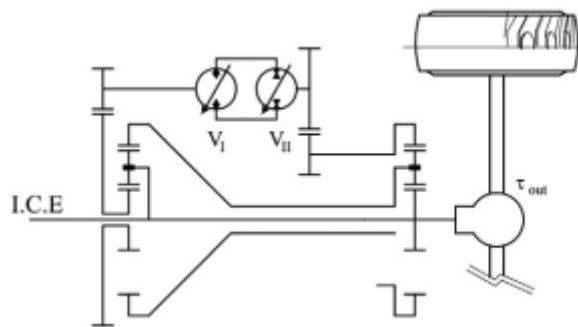


Figure 23: Compound coupled scheme. [1]

The presence of the two PGTs implies the presence of two “lockup points”, meaning that there are two speeds at which the power flows purely mechanically. One occurs when the speed of the planetary member connected to the primary unit has a null speed, and the other when the speed of the planetary member connected to the secondary unit has a null speed.

Figure 24 shows a scheme of the power flow in the transmission when the vehicle is at low speed, and the speed is smaller than the first lockup point. The hydraulic power is represented

by the red arrows while the mechanical is represented by the blue arrow. This scenario presents recirculation of power in the hydraulic path as well as in the mechanical path.

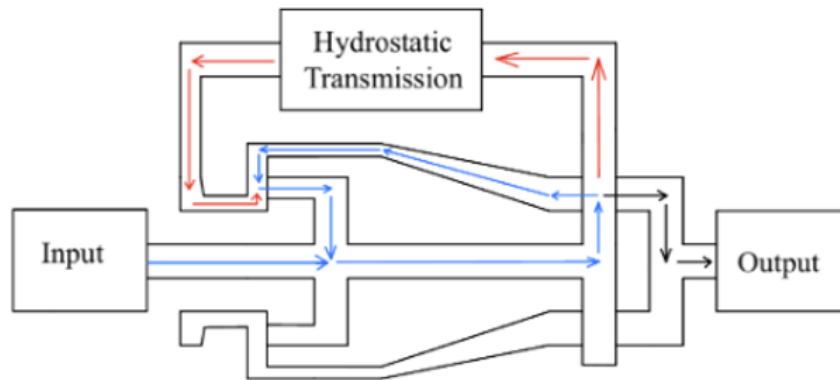


Figure 24: Power flow of the CC with the vehicle at a speed smaller than the first lockup point

For the scenario in which the vehicle operates in speeds between the two lockup points, there is no recirculation of power, as can be seen in the scheme in Figure 25, where the red arrows illustrate the hydraulic power, and the blue arrows illustrate the mechanical path.

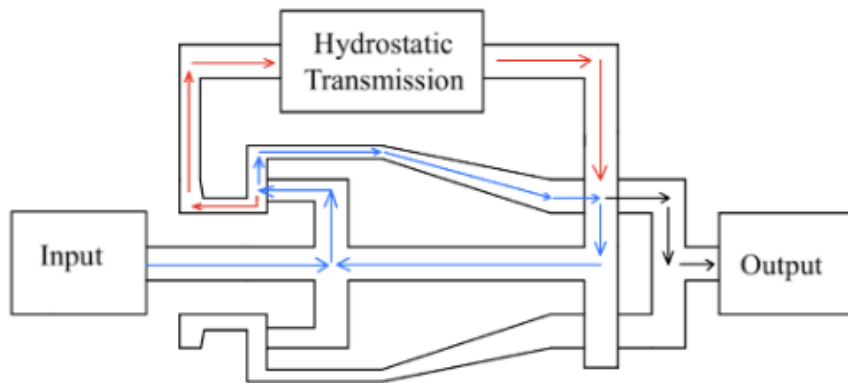


Figure 25: Power flow of the CC with the vehicle at a speed between the two lockup points

Moreover, if the vehicle operates at speeds greater than the second lockup point there is power recirculation, as illustrated in Figure 26.

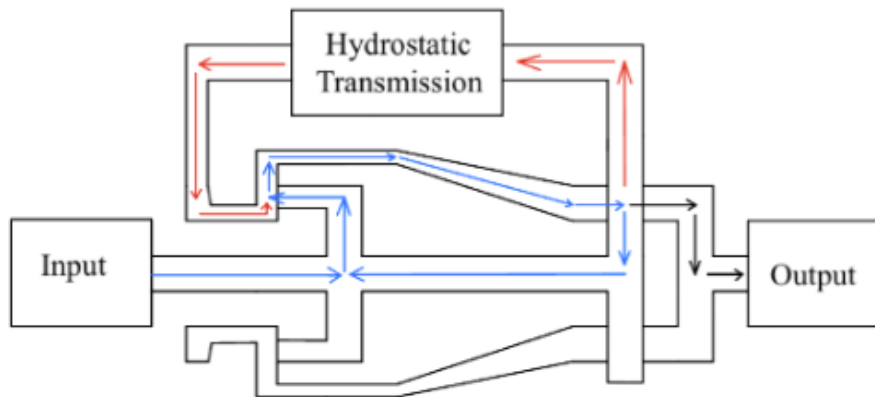


Figure 26: Power flow of the CC with the vehicle at a speed greater than the second lockup point

Similar to the previous configuration, the vehicle's speed is managed by adjusting the displacement of the hydraulic units. However, the compound-coupled architecture introduces greater complexity, making the behavior of the hydraulic units less straightforward compared to simpler configurations. Figure 27 illustrates an example of how the hydraulic units operate in this setup, where the dashed line represents the hydraulic units' displacement and the solid line represents the hydraulic units' speed. In this example, the vehicle accelerates from 0 to 120 km/h. Initially, the primary unit (Unit I) is at 0% displacement, while the secondary unit (Unit II) is at maximum displacement. Speed increases as Unit I's displacement rises, and after reaching its maximum, Unit II's displacement decreases to further increase the vehicle's speed.

The first lockup point occurs when Unit II reaches 0% displacement. At this point, all the power is transmitted mechanically. As the vehicle's speed increases, Unit II's displacement becomes increasingly negative until it reaches its maximum negative value. Afterward, the displacement of Unit I begins to decrease, eventually returning to 0%. At this stage, the second lockup point is achieved, and power is once again transmitted entirely through mechanical means.

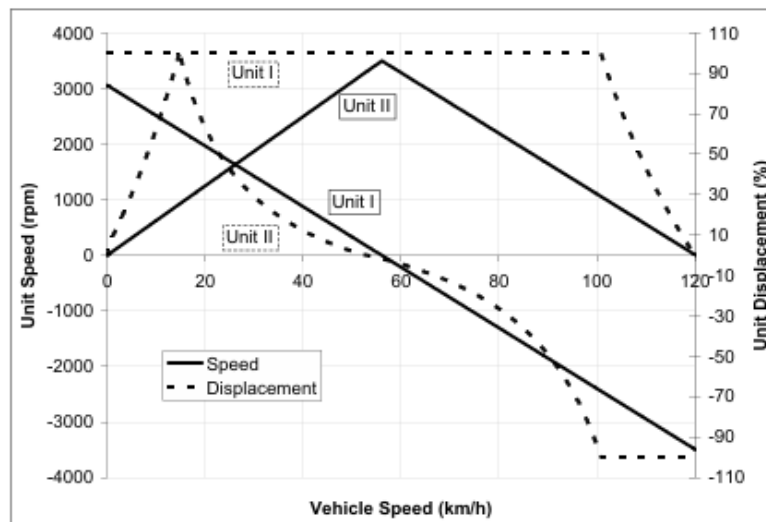


Figure 27: Compound coupled architecture hydraulic units operation [3]

## Chapter 3. Simulation Model

A series of simulations were performed using the software *Simcenter Amesim*, a multi-domain simulation software developed by Siemens, designed to help engineers model and analyze complex systems across various physical domains such as mechanical, electrical, thermal, and hydraulic.

The simulations were divided into two parts. In the first part, each configuration (IC, OC, and compound coupled) was simulated considering a constant load of 40 Nm. Afterward, the simulations were performed with the 2D longitudinal vehicle model, present in the *Simcenter Amesim*'s library, as load.

In this section, the main components of the hydromechanical transmission are characterized separately. The architectures of HMT differ by the position of the PGT, saying so, the same models were used in all architectures, although with different hydraulic unit sizing and gear ratios. It also presents the vehicle model used in the simulations as well as the control.

### 3.1. Hydrostatic Transmission Model

The model of a closed-circuit hydrostatic transmission used in the simulation is shown in

Figure 28. Composed of two variable displacement hydraulic units connected through two lines, whose maximum pressure is controlled by two relief valves (VL3) and is set to 300 bar.

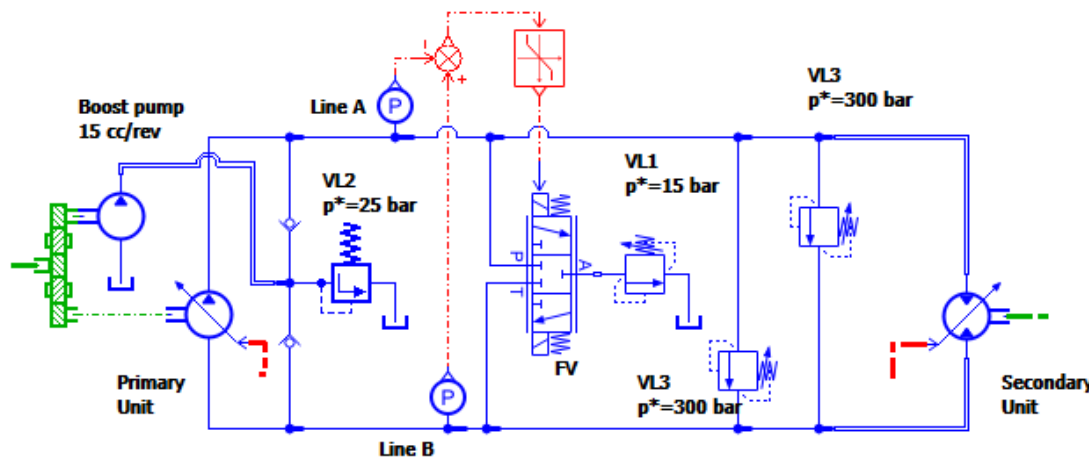


Figure 28: Simcenter Amesim model of the hydrostatic transmission

In a reversible system, both lines can assume the role of high-pressure line or low-pressure line. To ensure this, it is necessary to add a “flushing system.” Using a 3/3 directional control valve (FV), the low-pressure line is connected to an extra relief valve (VL1), that ensures its maximum pressure to 15 bar. The position of the FV is determined by the difference in pressure between lines B and A ( $B - A$ ), if the difference is negative, line B is the low-pressure line, and the valve opens the connection between ports A and T. If it's positive, line A is the low-pressure line, and the valve opens the connection between ports P and A.

Furthermore, the HST is also equipped with a boost pump, with a displacement of 15 cc/rev, whose role is to recover the lost flow and ensure that the low-pressure line is in a safe minimum pressure.

### 3.1.1. Planetary Gear Train

The planetary gear train used was the simple submodel with no inertia or losses present in *Amesim*'s library as shown in Figure 29. In it, ports 6 and 1 correspond to the sun gear, ports 5 and 2 are the planet/carrier gear, and ports 4 and 3 are the ring gear. The input velocities at ports 6 and 5 are passed without alteration to ports 1 and 2, while the output velocity at ports 3 and 4 is computed respecting the Willis equation (See eq. 2), where:

- $\omega_{port_6} = \omega_{port_1} = \omega_s$
- $\omega_{port_3} = \omega_{port_4} = \omega_R$
- $\omega_{port_5} = \omega_{port_2} = \omega_C$

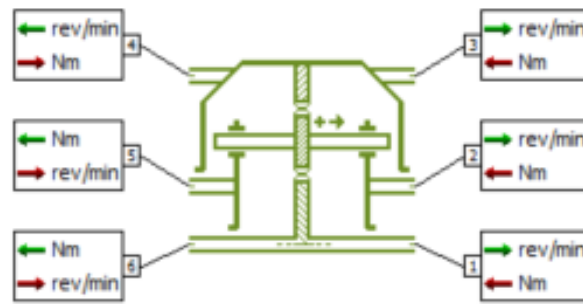


Figure 29: Simcenter Amesim's planetary geartrain model

The output torques at ports 5 and 6 are computed using eq. (15) and eq. (14) respectively.

$$T_6 = \frac{T_3 - T_4}{\tau_0} + T_1 \quad (14)$$

$$T_5 = \frac{\tau_0 - 1}{\tau_0} \cdot (T_3 - T_4) + T_2 \quad (15)$$

Where  $\tau_0$  is the gear ratio (see eq. 3),  $T_1, T_2, T_3$ , and  $T_4$  are the input torque in ports 1, 2, 3, and 4 respectively.

### 3.1.2. Gear Models

In the simulations, two types of gear models were employed: a 3-port gear model and a 4-port gear model, and a reducer.

- **3-port gear model**

The model is illustrated in Figure 30, where ports 2 and 3 are rotary, while port 1 is linear. The rotary velocity at ports 2 and 3 are equal ( $\omega_1 = \omega_2$ ). The linear velocity at port 1 ( $v$ ) is proportional to the gear radius ( $R$ ), as shown in eq. (16). Furthermore, the force ( $F$ ) at port 1 is

given by the relationship shown in eq. (17),  $T_2$  and  $T_3$  are the torque at ports 2 and 3 respectively. No losses were considered.

$$v = -R \cdot \omega_2 \quad (16)$$

$$T_2 = T_3 + R \cdot F \quad (17)$$

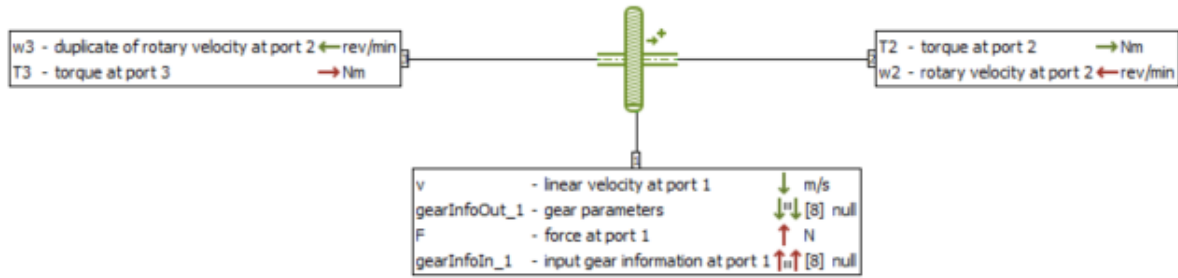


Figure 30: Simcenter Amesim's 3-port gear model

- **4-port gear model**

Figure 31 provides a schematic representation of the model, where ports 2 and 4 are rotary, while ports 1 and 3 are linear. The linear velocities at ports 1 and 3 are equal but have opposite signs ( $v_1 = -v_3$ ). The relationship between the rotary velocities at ports 2 and 4 and the linear velocity is described in eq. (18), where  $R$  is the gear radius. Additionally, the force at port 3 is given by eq. (19), where  $F_1$  is the force at port 1, and  $T_2$  and  $T_4$  are the torque at ports 2 and 4 respectively. No losses were considered in this model.

$$\omega_2 = -\omega_4 = \frac{v_1}{R} \quad (18)$$

$$F_3 = \frac{T_2 - T_4}{R} - F_1 \quad (19)$$

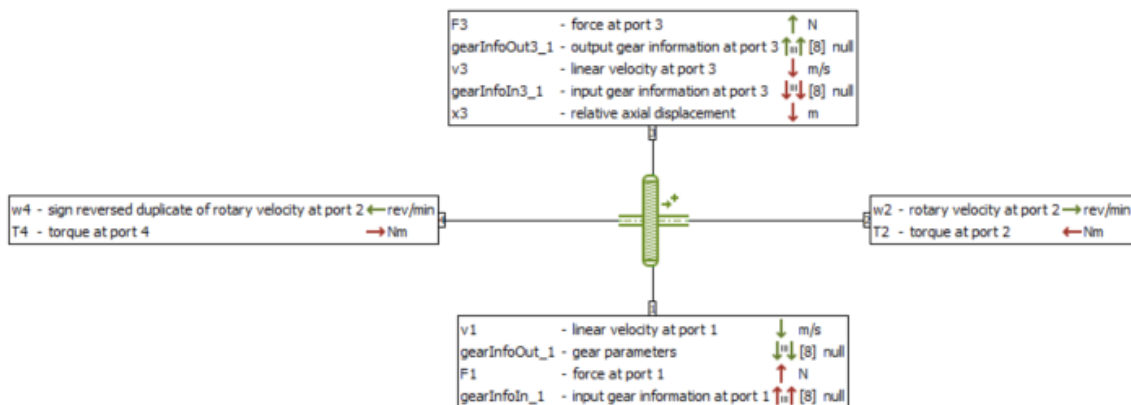


Figure 31: Simcenter Amesim's 4-port gear model

- **Reducer**

The reducer model, illustrated in Figure 32, represents an ideal rotary mechanical gear system. It operates with a fixed gear ratio ( $\alpha$ ), which defines the relationship between the port 1 and port 2 rotary velocities ( $\omega_1$  and  $\omega_2$ ) and torques ( $T_1$  and  $T_2$ ), as shown in eqs. (20) and (21). This model assumes 100% mechanical efficiency, meaning there are no losses due to friction, heat, or other factors.

$$\omega_2 = \alpha \cdot \omega_1 \quad (20)$$

$$T_1 = \alpha \cdot T_2 \quad (21)$$

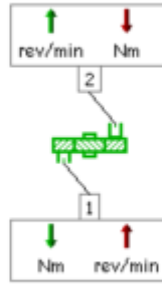


Figure 32: Simcenter Amesim's Reducer model

### 3.1.3. Vehicle Model

The vehicle model used in this work is shown in Figure 33, a simple dynamic model of a 2 axles vehicle. In it, ports 1 and 3 are braking signal inputs for the rear and front axles respectively, throughout this study the signal is equal to zero. Ports 2 and 4 are the driving torque input, the transmission's output shaft is connected to port 2, while port 4 is connected to a zero-torque source. To define the slope of the road a signal with the percentage of the slope, in which 100% is equal to  $45^\circ$ , is connected to port 5. The wind velocity is added in port 6, which is considered zero in this study. Ports 7, 8, and 9 are output signals in which is possible to acquire the distance traveled by the vehicle, the vehicle's longitudinal velocity, and acceleration respectively.

The simulations were performed using the road configuration without slip and rear wheel drive. The vehicle characteristics adopted for all simulations are described in Table 1 and Table 2 shows the aerodynamics and rolling parameters.

Table 1: Vehicle characteristics

Parameter	Value	Unit
Mass	11000	[kg]
Rear wheel radius	0.934	[m]

Table 2: Aerodynamics and rolling parameters

Parameter	Value	Unit
Rolling resistance coefficient	0.02	[-]
Air density	1.226	$[kg/m^3]$
Drag coefficient	0.9	[-]
Frontal area	4	$[m^2]$

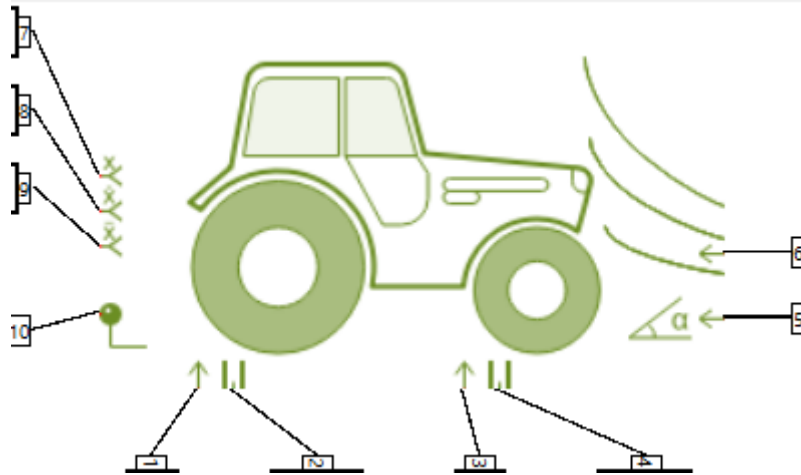


Figure 33: Simcenter Amesim's longitudinal vehicle model

### 3.1.4. Control

The control strategy employed in the simulation is based on a PID (Proportional-Integral-Derivative) controller, which regulates the displacements of the hydraulic units to maintain the desired vehicle speed, schematized in Figure 34. The input to the PID controller is the target speed profile, item 1, set in  $km/h$ , in item 2 the signal is converted to  $m/s$ , which is compared with the actual vehicle speed measured from the simulation, item 4. The error between the target and actual speeds is used by the PID controller, item 3, to generate an output signal that adjusts the displacements of the primary (item 6) and secondary (item 7) hydraulic units. In item 5 the sequential control of the displacements is set according to the graph in Figure 35 for the output coupled and Figure 36 for the input coupled. The controller continuously modifies these displacements to minimize the speed error, ensuring that the vehicle follows the target speed profile as closely as possible.

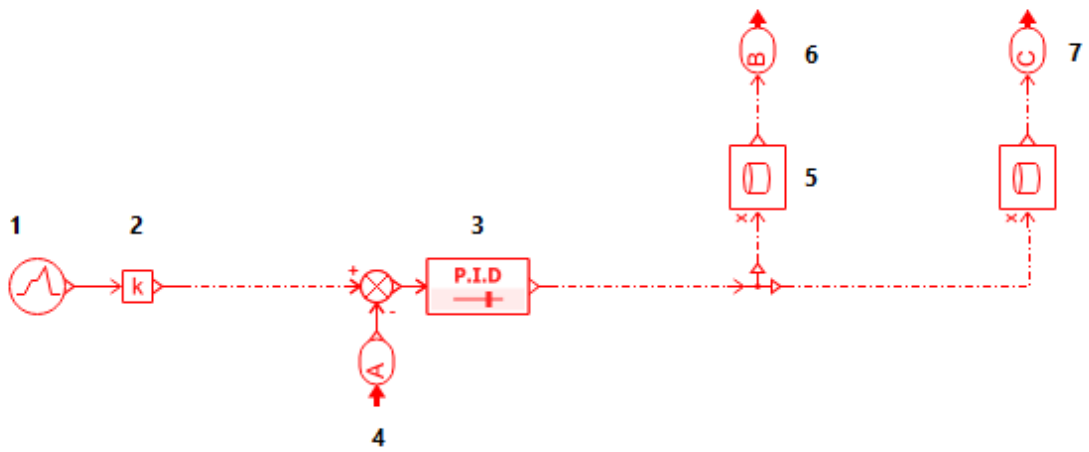


Figure 34: Model of the PID control

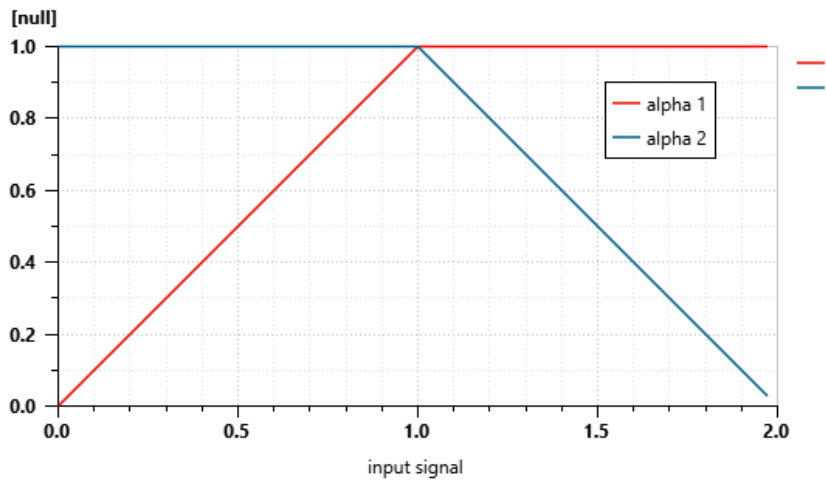


Figure 35: OC Sequential displacement control

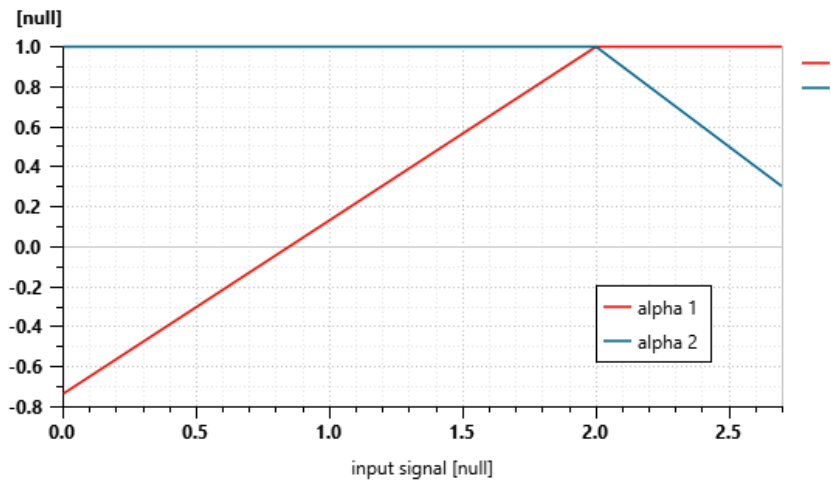


Figure 36: IC Sequential displacement control

## Chapter 4. Constant Load Simulations

This chapter presents the results and analysis of the constant load simulations for both input-coupled and output-coupled hydromechanical transmission configurations. This test case provides a fundamental understanding of the power split in each configuration without the complexities of variable load or control strategies. It was assumed that mechanical and hydraulic components were ideal and thermal effects were neglected.

### 4.1. Simulation Setup

For these simulations, a constant load of 40Nm was applied to the transmission's output shaft. The output shaft's speed is controlled by controlling the displacements of the hydraulic units linearly. The key parameters used in the transmissions are listed in Table 3 and the output-coupled model schematic is shown in Figure 37 and the input-coupled in Figure 38.

Table 3: Constant load simulation parameters

	Parameter	Value	Unit
Output Coupled	ICE speed	2200	[RPM]
	Primary HU displacement	80	[ $cm^3/rev$ ]
	Secondary HU displacement	80	[ $cm^3/rev$ ]
	PGT gear ratio ( $\tau_0$ )	-1.91	[-]
	Transmission Ratio ( $i_1$ )	1.4	[-]
Input Coupled	ICE speed	2200	[RPM]
	Primary HU displacement	80	[ $cm^3/rev$ ]
	Secondary HU displacement	80	[ $cm^3/rev$ ]
	PGT gear ratio ( $\tau_0$ )	-5.0	[-]
	Transmission Ratio ( $i_1$ )	1.77	[-]
	Transmission Ratio ( $i_2$ )	3.6	[-]

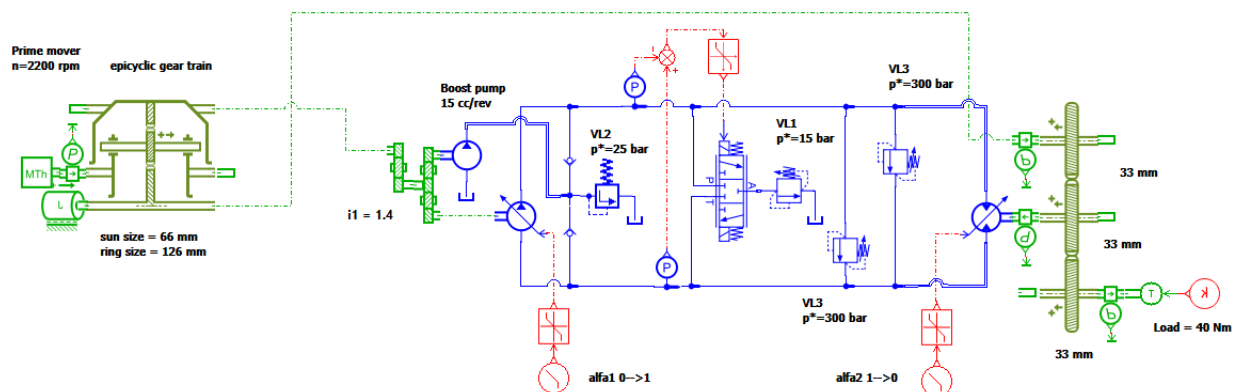


Figure 37: OC constant load simulation model schematics

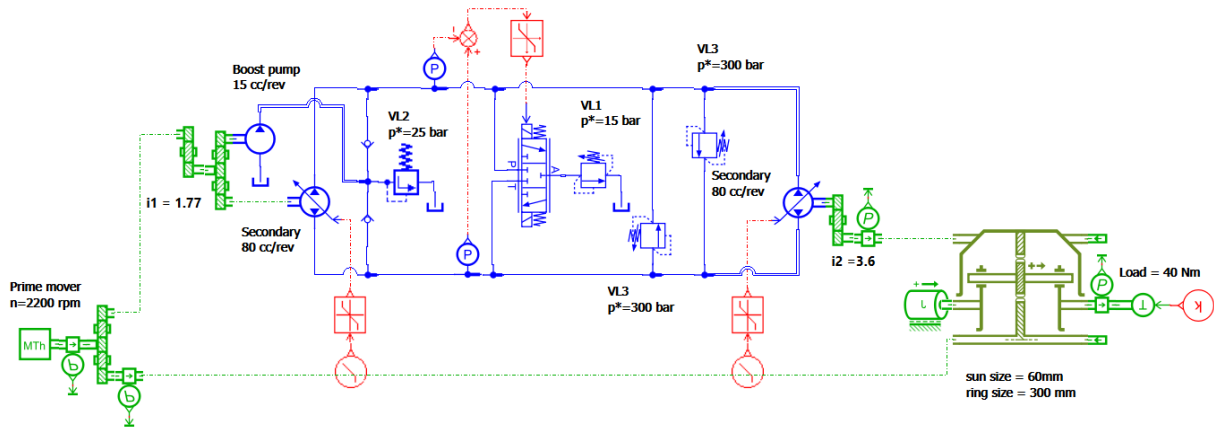


Figure 38: IC constant load simulation model schematics

The simulations were conducted over 50 seconds, generating 5001 data points. To perform it, the displacements of the hydraulic machines were changed one at a time. In the OC case, at the start, the primary unit has zero displacement ( $\alpha_1 = 0$ ) while the secondary is at maximum displacement ( $\alpha_2 = 1$ ). In the first 10 seconds of simulation both displacements are constant, then the displacement of the primary unit is increased linearly until reaching its maximum displacement ( $\alpha_1 = 1$ ). After that, the displacement of the secondary unit is decreased linearly until reaching zero displacement as shown in Figure 39.

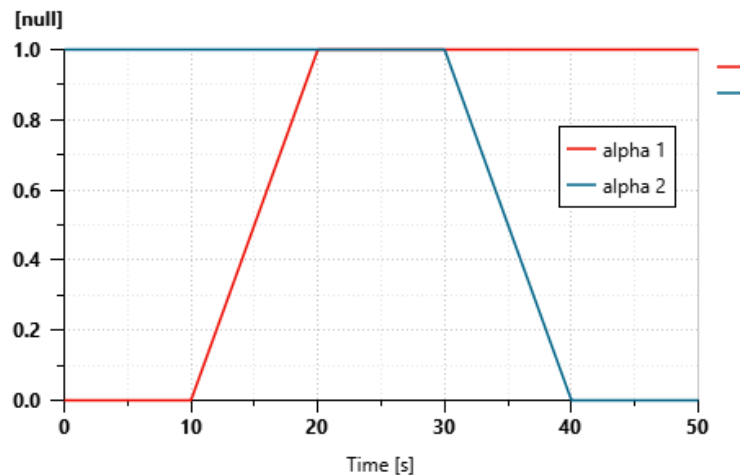


Figure 39: OC displacement control

In the IC case, at the start, the primary unit had a negative displacement while the secondary unit was fully engaged at maximum displacement ( $\alpha_2 = 1$ ). For the first 10 seconds, these displacements remained constant. Afterward, the primary unit's displacement was gradually increased to its maximum ( $\alpha_1 = 1$ ). Once the primary unit reached full displacement, the secondary unit's displacement decreased linearly, reaching a minimum displacement by the end of the simulation, as shown in Figure 40.

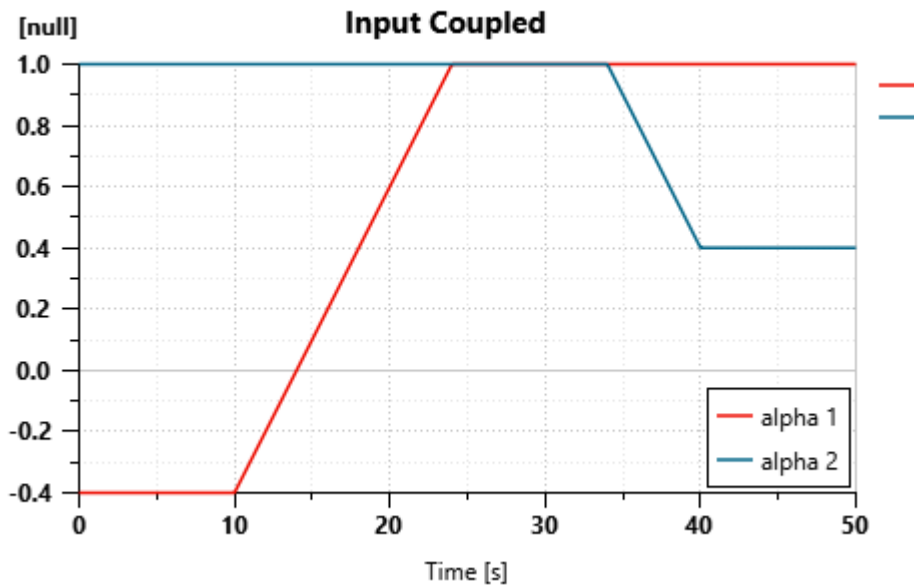


Figure 40: IC displacement control

## 4.2. Results

The main focus of this simulation was to observe the power distribution between hydraulic and mechanical components throughout the operation. Figure 41 and Figure 42 illustrates the power ratio of the OC and IC respectively, with the red line representing the percentage of hydraulic power and the blue line showing the proportion of mechanical power. This distribution provides a clear picture of how both configurations handle power under constant load conditions.

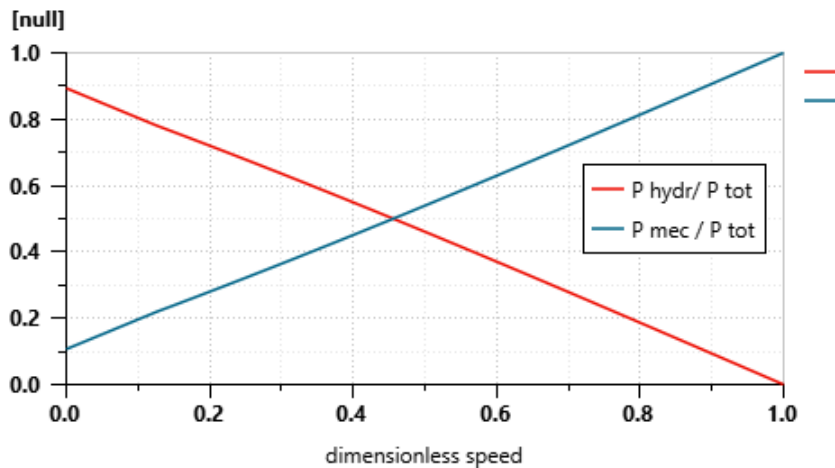


Figure 41: OC constant load power ratio

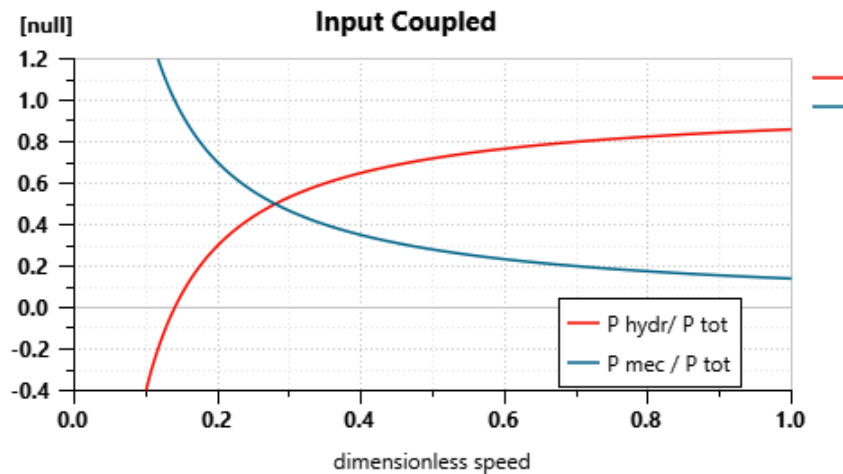


Figure 42: IC constant load power ratio

It is possible to observe that the input-coupled configuration exhibits an opposite behavior compared to the output-coupled system in terms of power distribution. At low speeds, the IC configuration shows the mechanical power higher than the hydraulic power, in fact, at very low speeds the hydraulic power is negative which means there is recirculation of power. As the vehicle speed increases, the proportion of mechanical power decreases, while the hydraulic power contribution rises, demonstrating a shift in how the transmission handles power at different speeds. This behavior contrasts with the output-coupled configuration, where the hydraulic power is typically more dominant at lower speeds and reduces as the speed increases.

Figure 43 shows how torque is distributed along the hydraulic and mechanical path. On the left side is the IC configuration and it is possible to see that independently of the output shaft's speed the torque is majorly hydrostatic. On the right side, the output coupled configuration, at low speeds the torque is mostly hydraulic but as the speed increases, the torque shifts from hydrostatic to mechanical.

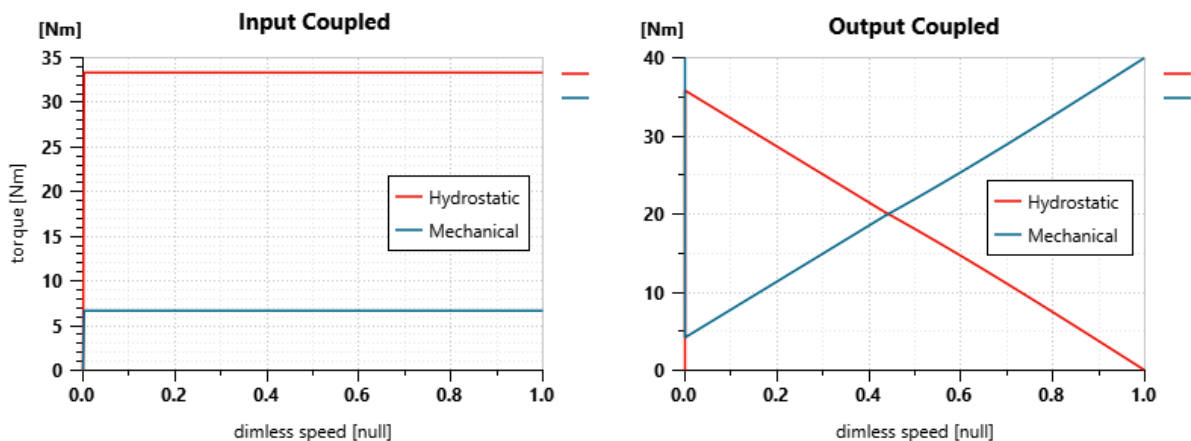


Figure 43: IC and OC transmission torque

## Chapter 5. Vehicle Model Simulations

The following simulations were performed aimed to evaluate the performance of the HMT using the vehicle model described in section 3.1.3, where the parameters used can also be found. This simulation represented a more realistic scenario where the transmission system was integrated into a vehicle dynamics model, allowing the analysis of system behavior under load while considering the vehicle's overall dynamics. It was assumed that mechanical and hydraulic components were ideal and thermal effects were neglected.

### 5.1. Simulation Setup

The following simulations were performed by controlling the HU displacements linearly as shown in Figure 44, where the solid lines represent the OC scenario's displacement control, and the dashed lines represent the IC scenario's. This approach allowed the system to adjust dynamically and achieve a final speed based on the displacement of the hydraulic units and the overall system response.

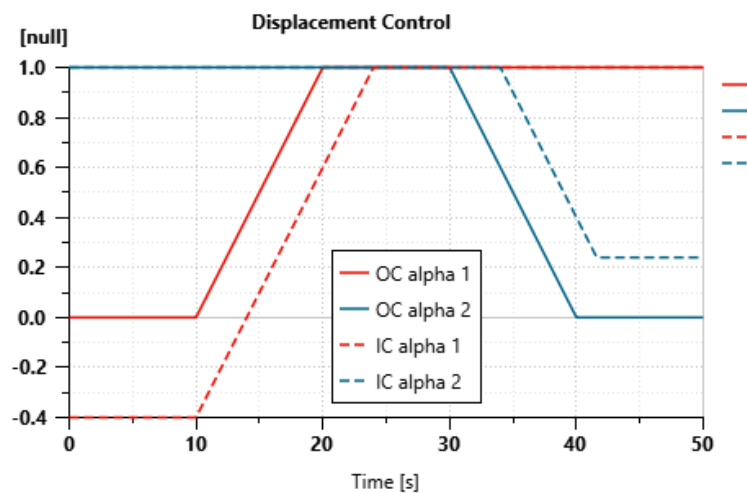


Figure 44: Displacement control

The key parameters for the hydromechanical transmission are listed in Table 4 and the model schematic for the OC and IC configurations are shown in Figure 45 and Figure 46 respectively. The transmission ratios used were chosen to reach a maximum vehicle's speed of 41km/h and the final transmission's efficiency was not considered.

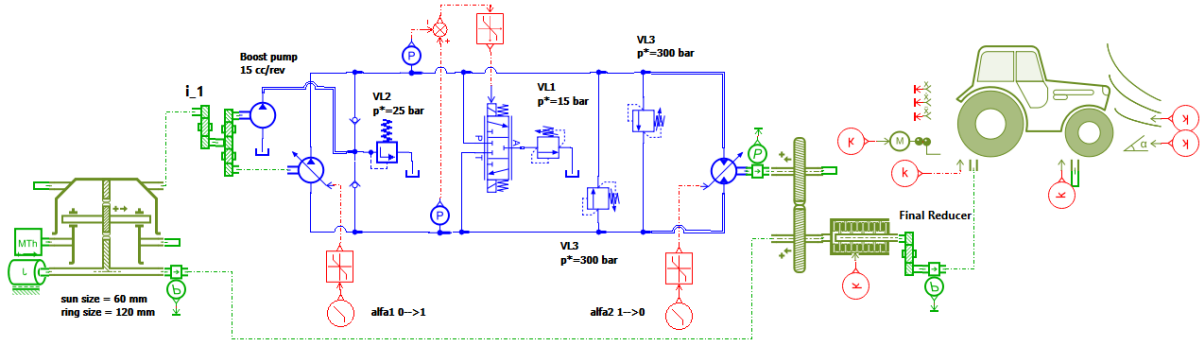


Figure 45: OC vehicle model simulation schematics

Table 4: Vehicle model simulation parameters

	Parameter	Value	Unit
<b>Output Coupled</b>	ICE speed	2200	[RPM]
	Primary HU displacement	80	[ $cm^3/rev$ ]
	Secondary HU displacement	80	[ $cm^3/rev$ ]
	PGT gear ratio ( $\tau_0$ )	-2.0	[-]
	Transmission ratio ( $i_1$ )	1.4	[-]
	Final Reducer	56.5	[-]
<b>Input Coupled</b>	ICE speed	2200	[RPM]
	Primary HU displacement	80	[ $cm^3/rev$ ]
	Secondary HU displacement	80	[ $cm^3/rev$ ]
	PGT gear ratio ( $\tau_0$ )	-5.0	[-]
	Transmission ratio ( $i_1$ )	1.77	[-]
	Transmission ratio ( $i_2$ )	2.6	[-]
	Final Reducer	20	[-]

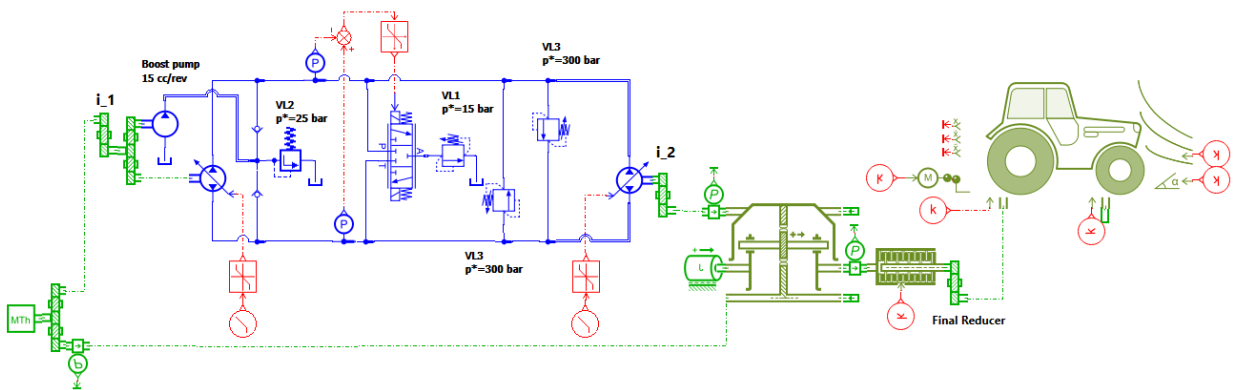


Figure 46: IC vehicle model simulation schematics

## 5.2. Results

### 5.2.1. Vehicle Speed Response

The vehicle's speed profiles for the output-coupled (OC) and input-coupled (IC) configurations are shown in Figure 47. The OC configuration, represented by the solid line, exhibits higher acceleration during the initial phase, with more subtle acceleration as the displacement approaches 100%. In contrast, the IC configuration (dashed line) displays a more linear acceleration throughout the displacement change of the primary unit. Both configurations experience significant acceleration when the secondary unit's displacement reaches its minimum, with the IC configuration showing a greater acceleration during this phase.

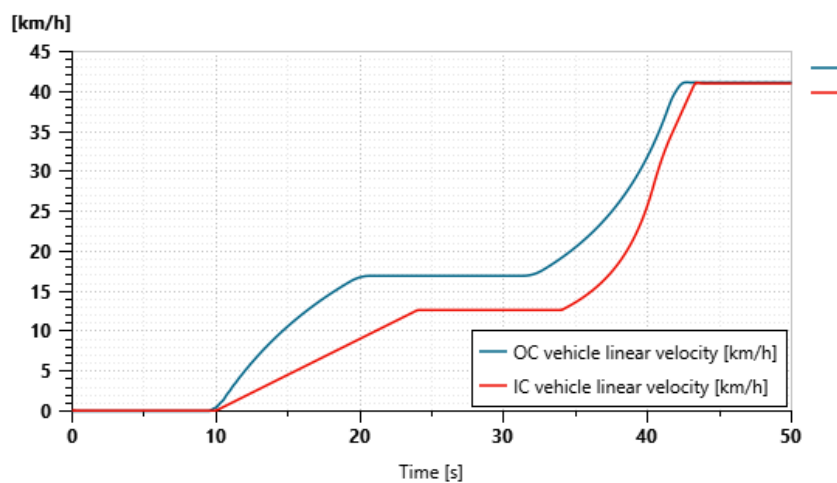


Figure 47: Speed profiles of vehicle model simulation

### 5.2.2. Output Torque

In this scenario, the vehicle is running on a flat surface, no slope is applied. The output torque profiles for both the output-coupled (OC) and input-coupled (IC) configurations are shown in Figure 48. In the OC configuration, torque increases significantly during the initial phase, particularly when the displacement of the primary hydraulic unit is low. As the displacement approaches its maximum value, the torque levels off, indicating a more stable transmission response. In contrast, the IC configuration demonstrates a more linear torque response but experiences a higher torque peak, during the transition of the secondary hydraulic unit's displacement, leading to a more aggressive torque increase compared to the OC setup.

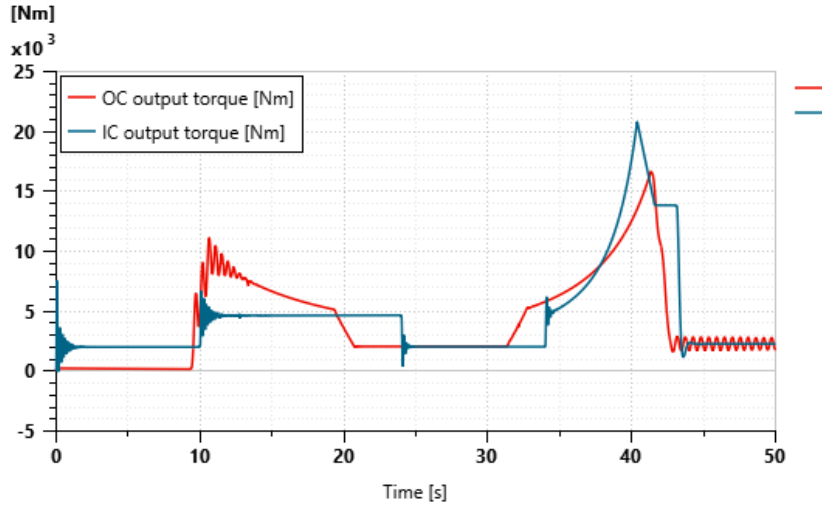


Figure 48: Torque profile at the transmission's output shaft

Additionally, Figure 49 illustrates the torque distribution between the mechanical and hydrostatic paths. In the OC configuration, mechanical torque gradually increases with speed, while the hydrostatic contribution dominates at lower speeds. For the IC configuration, the mechanical power is more prominent at low speeds, but the hydrostatic path plays a greater role as the vehicle accelerates. This transition affects the torque behavior, with the IC configuration showing more pronounced changes in torque distribution at various speeds.

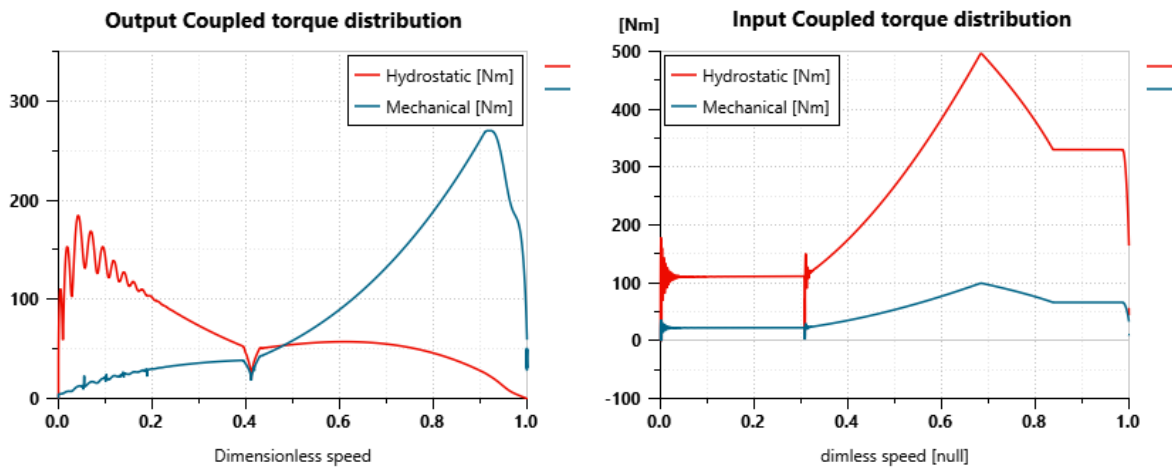


Figure 49: OC and IC torque distribution

### 5.2.3. Power Ratio

As illustrated in Figure 50, the OC configuration shows a dominant hydrostatic power contribution at lower speeds, which transitions to a higher mechanical power contribution as speed increases. This indicates a smooth power transfer as the vehicle accelerates. Conversely, the IC configuration exhibits a more dynamic power shift, with mechanical power initially prevailing at low speeds, while hydrostatic power becomes increasingly significant as acceleration continues. This distinct behavior highlights the differences in how each configuration manages power during operation.

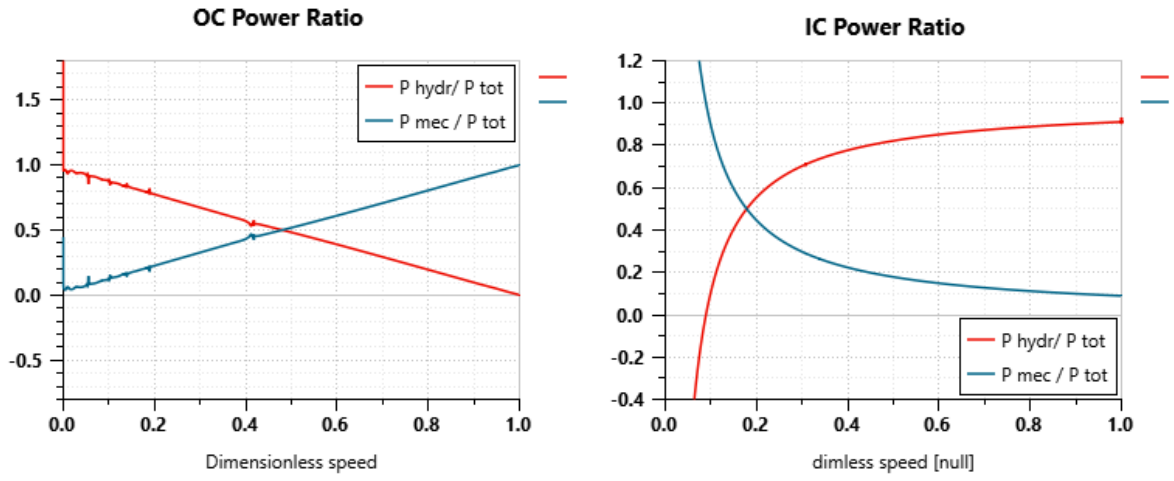


Figure 50: OC and IC power ratio

## Chapter 6. PID Control Simulation

In this chapter, it is explored the use of a Proportional-Integral-Derivative (PID) control strategy to regulate the vehicle's speed by controlling the displacements of the hydraulic units in the hydromechanical transmission.

### 6.1. Simulation Setup

The simulation setup for the following simulations was based on the same parameters as the previous simulations, presented in Chapter 5. The vehicle model was the same, using the properties in section 3.1.3 and the hydromechanical transmission has the properties presented in Table 4.

For this set of simulations, the control shown in section 3.1.4 was added to the plant (see Appendix). In contrast with the previous chapter, the input for the simulation is the desired speed profile shown in Figure 51 while the displacements of the hydraulic units are the output of the PID control.

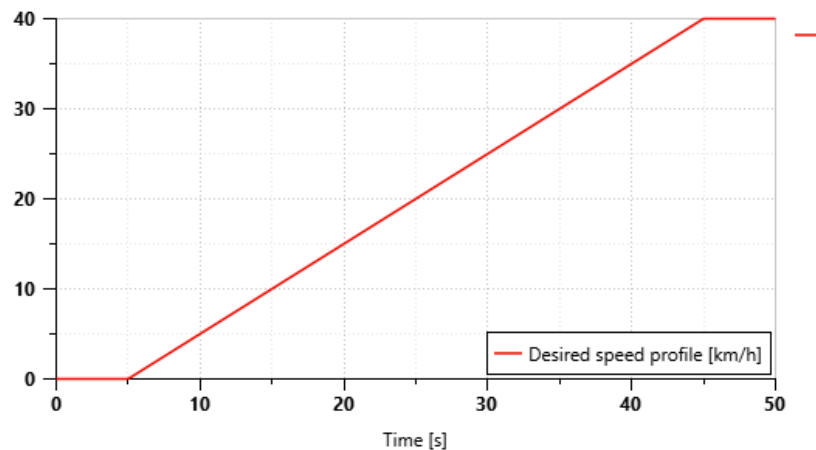


Figure 51: Requested speed profile

## 6.2. Results

### 6.2.1. Vehicle Speed Response and Displacement Control

The vehicle speed response under PID control shows notable enhancements in tracking the desired speed profile. Figure 52 illustrates the speed trajectory, where the solid line indicates the actual speed achieved in the output-coupled case and the input-coupled case. The PID controller effectively responds to the desired mission in both scenarios.

Displacement control profiles, depicted in Figure 53, demonstrate how the hydraulic unit adjustments are finely tuned to maintain the desired speed. Where the solid lines indicate the displacements of the OC case, and the dashed lines are the ones of the IC case. The PID control ensures a precise correlation between displacement changes and speed variations.

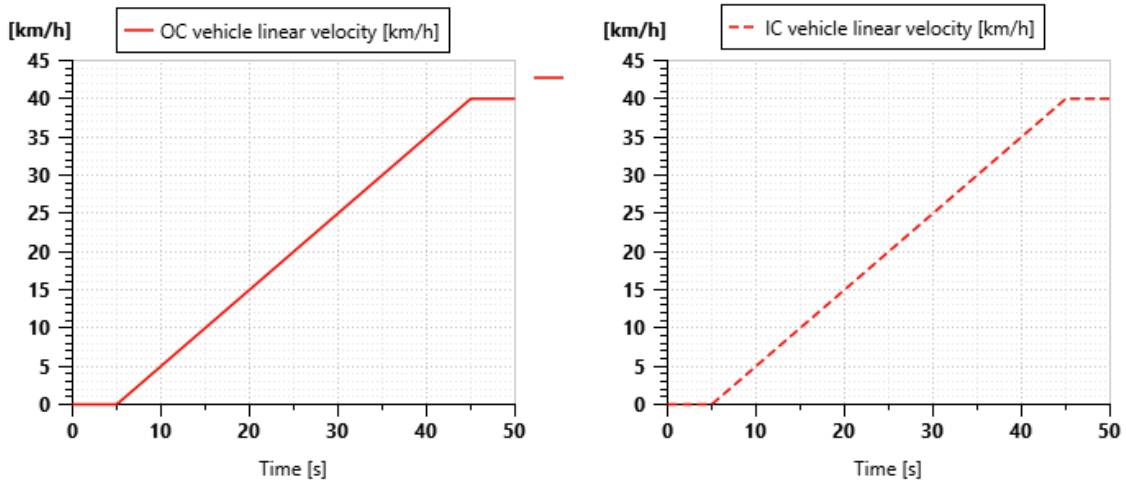


Figure 52: Vehicle's linear velocity response

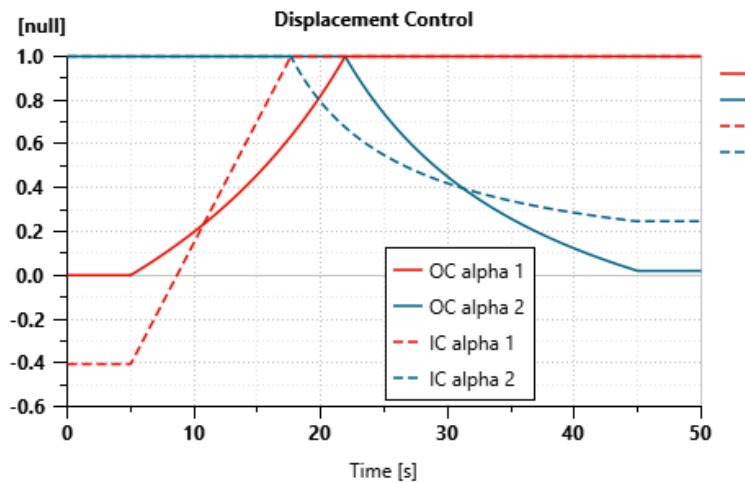


Figure 53: Hydraulic units' displacement

### 6.2.2. Output torque

Due to the constant acceleration requested in this scenario, the output torque shown in Figure 54 is almost constant. The slight increase in output torque is primarily attributed to overcoming aerodynamic drag. Furthermore, as the vehicle model simulated is the same for the OC and IC, the output torque profile is almost the same.

The torque in the IC configuration is greater than in the OC configuration when the vehicle is stationary due to the differences in how each system engages the hydraulic units. In the IC setup, the hydraulic pump is directly connected to the engine, allowing for greater torque transmission from the engine at low speeds or when stationary. In contrast, the OC configuration relies on the power generated from the hydrostatic transmission, which may not provide as much torque when the vehicle is not moving.

For the OC configuration, the torque distribution exhibits a linear transition: as speed increases, the amount of torque provided by the hydrostatic path gradually decreases, while the

mechanical path compensates by delivering progressively more torque. In contrast, the IC configuration maintains a consistent torque output from both the hydrostatic and mechanical paths throughout the entire speed range. In this setup, the hydrostatic system provides more than 80% of the total required torque, with the mechanical path contributing the remaining portion. Figure 55 illustrates these distinct torque distributions, emphasizing how each configuration uniquely manages torque delivery.

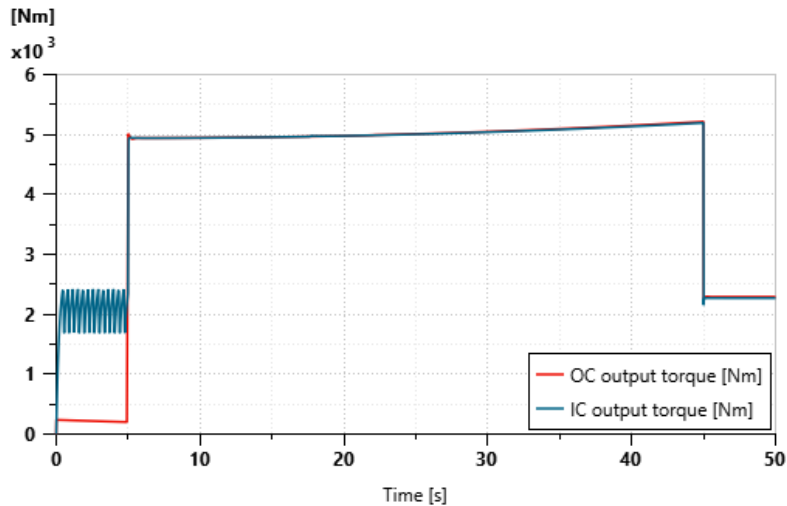


Figure 54: Output shaft's torque

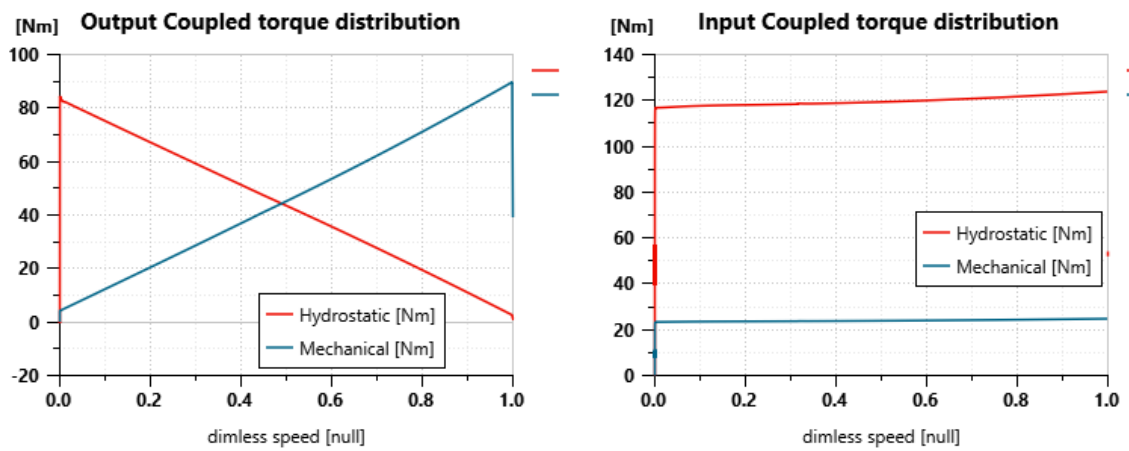


Figure 55: OC and IC torque distribution

### 6.2.3. Power ratio

In the OC configuration, the power ratio between hydrostatic and mechanical paths shifts progressively as speed increases. Initially, the hydrostatic path provides the majority of the power needed to meet the acceleration demands. However, as the vehicle gains speed, mechanical power gradually takes over a larger share of the total power, while the hydrostatic power contribution decreases.

In the IC configuration, however, the power behavior differs showing power recirculation at low speeds. During this phase, hydrostatic power is negative, indicating that power is being

recirculated within the system rather than contributing directly to forward propulsion. As the vehicle accelerates and speed increases, hydrostatic power gradually shifts from negative to positive values and continues to increase.

Figure 56 illustrate these power distribution trends, and emphasize the unique power flow in each configuration, reflecting their distinct approaches to handling power demands across the speed range.

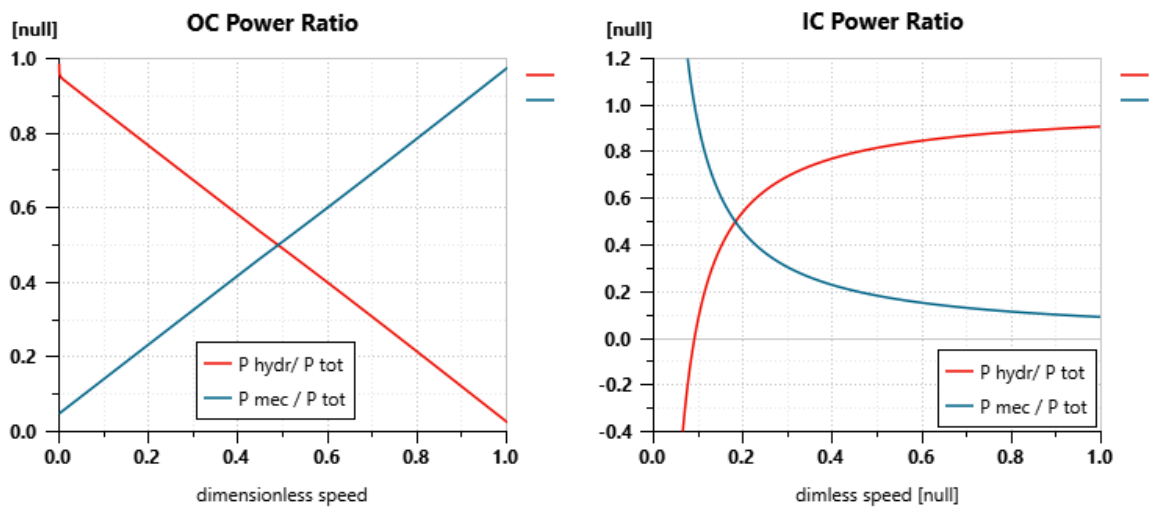


Figure 56: OC and IC power ratio

## Chapter 7. Vehicle on Slopes

The simulations for the vehicle on slopes were conducted for both output-coupled and input-coupled configurations, focusing on the vehicle's performance under positive and negative slope conditions. Each slope case was divided into two sub-cases: low-speed and high-speed scenarios. The key parameters for these simulations were kept consistent with the previous configurations, with the only variable being the slope change.

### 7.1. Simulation Setup

Before starting the proper simulation, the PID control model was run to determine the hydraulic units' displacement profiles for the desired speeds, 15 km/h for low-speed case and 40 km/h for high-speed. As can be observed in Chapter 5, linearly varying the displacement results in high acceleration and, consequently, high torque, which can increase pressure within the hydrostatic transmission. This pressure may cause the regulation of the relief valve.

The goal of this analysis is to observe the performance of the transmission under the increasing torque caused by the slope, for this reason, the displacement profiles obtained from the simulation with the PID control were saved and used as input for this set of simulations aiming to obtain a controlled acceleration of the vehicle. The displacement profiles obtained are shown in Figure 57 and Figure 58 for the output coupled and input coupled respectively, where the left side is the one used in the low-speed scenarios and the right side is the one used for high-speed scenarios. This control is used either for the positive slope or the negative slope.

#### 7.1.1. Positive Slope

- Low Speed:
  - Phase 1: The vehicle goes from 0 to 15 km/h at constant acceleration on a flat surface (0% slope).
  - Phase 2: Once the vehicle reaches 15 km/h, the displacements are held constant, and the slope gradually increases from 0% to 30%.
- High Speed:
  - Phase 1: The vehicle accelerated from 0 to 40 km/h at constant acceleration on a flat surface (0% slope).
  - Phase 2: At 40 km/h, the displacements are held constant, and the slope increases from 0% to 30%.

#### 7.1.2. Negative Slope

- Low Speed:
  - Phase 1: The vehicle accelerated from 0 to 15 km/h at constant acceleration on a flat surface (0% slope).
  - Phase 2: After reaching 15 km/h, the slope decreased from 0% to -30%, simulating a downhill scenario while maintaining the constant displacement.
- High Speed:

- Phase 1: The vehicle accelerated from 0 to 40 km/h at constant acceleration on a flat surface (0% slope).
- Phase 2: With the vehicle at 40 km/h, the slope was reduced from 0% to -30%, and the displacement was kept constant.

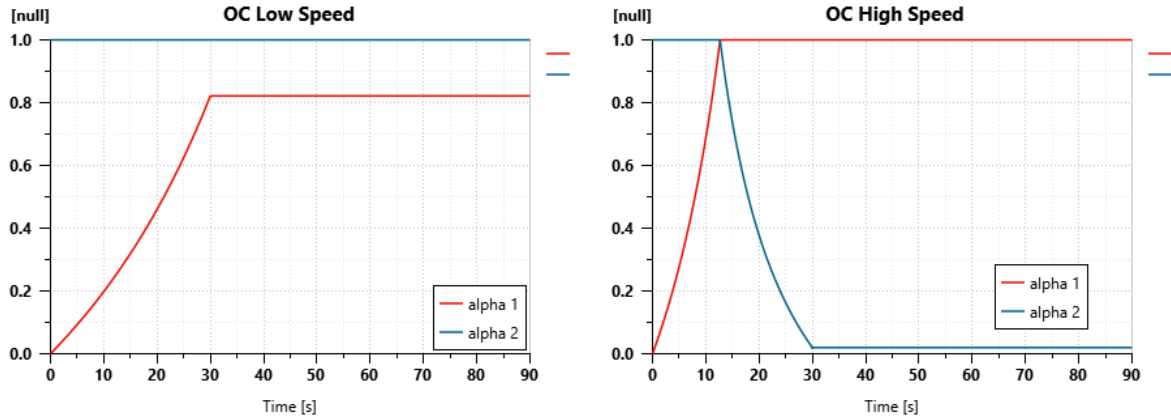


Figure 57: OC displacement control on slope

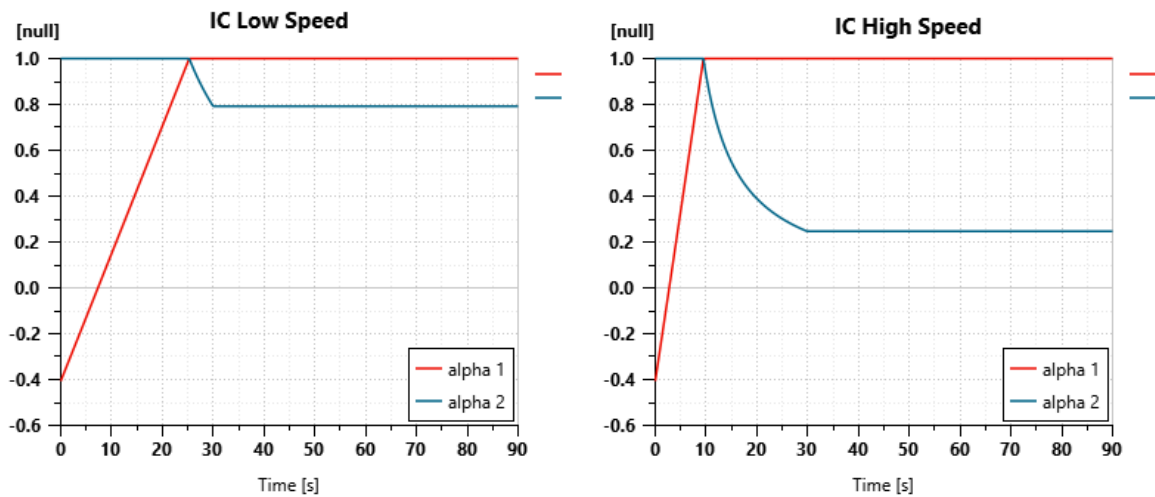


Figure 58: IC displacement control on slope

## 7.2. Output Couple Results

This section discusses the vehicle's performance on positive and negative slopes for the output-coupled (OC) configuration. The focus is on low and high-speed simulations, highlighting variations in vehicle speed, pressure drop across the hydraulic system, and power distribution between the mechanical and hydrostatic paths. The results examine how the transmission responds to changes in slope.

### 7.2.1. Low speed

During the low-speed simulation on a slope, there is a slight increase in vehicle speed when descending a negative slope and a slight decrease when ascending a positive slope, as illustrated in Figure 59, where the dashed black line represents the reference vehicle at 0% slope. The

system maintains control of the speed effectively, and there is no engagement of the relief valve during these conditions, as can be seen in Figure 60 there is no flow rate through the relief valve, indicating that the transmission is functioning within its pressure limits.

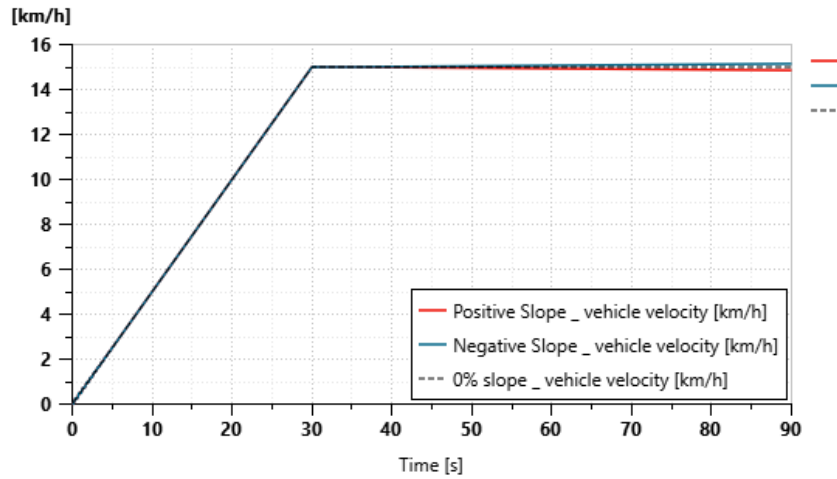


Figure 59: OC low speed \_ vehicle speed on a slope

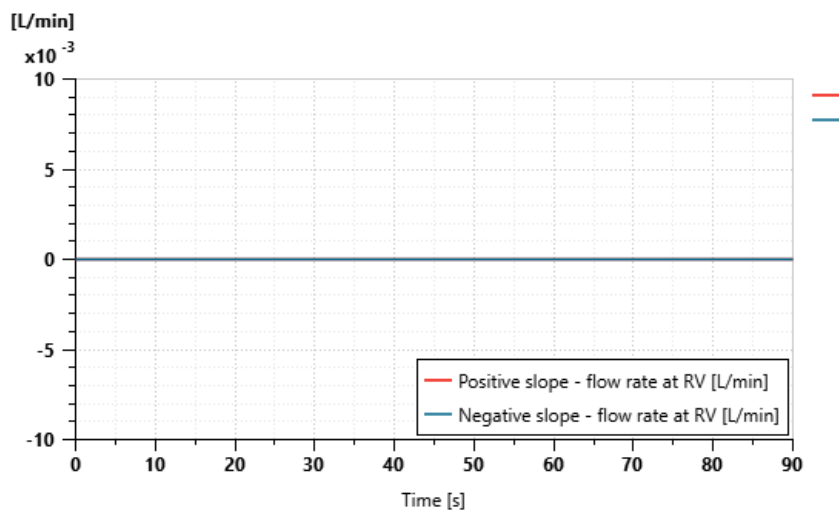


Figure 60: OC low speed \_ flow rate through the relief valve

The hydrostatic transmission is a reversible system in which both hydraulic units are capable of operating either as a pump or as a motor. When the vehicle is moving forward or is submitted to a positive slope the vehicle is under positive torque, on the other hand when moving in reverse or submitted to a negative slope, the vehicle is under negative torque.

In Figure 61 it is possible to observe the change between the high-pressure and low-pressure lines. The reference dashed line, where the vehicle is moving forward at 0% slope, and the positive slope, marked by the red line, the pressure drop is always positive. On the negative slope (blue line), while the vehicle increases speed, the pressure drop remains positive. However, as the vehicle begins to descend, the pressure drop decreases and eventually becomes negative when the high and low-pressure lines reverse, reflecting a change in the hydraulic unit's operation.

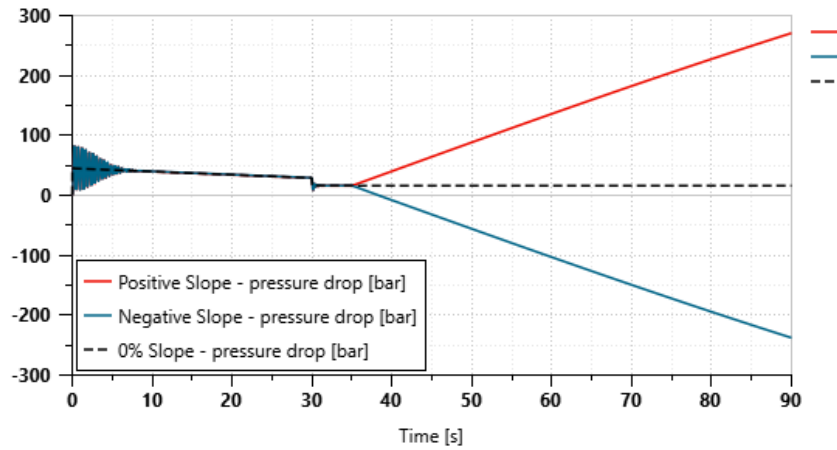


Figure 61: OC low speed \_ pressure drop between high and low-pressure lines

Figure 62 shows the power distribution along the hydrostatic and mechanical paths for the scenarios of positive and negative slopes. The power ratio exhibits different behaviors on positive and negative slopes. On the positive slope, the hydrostatic power remains dominant, with mechanical power increasing gradually as the vehicle moves uphill.

On the negative slope, the OC configuration responds similarly to an input-coupled system, with a significant portion of power recirculated through the hydrostatic path as the vehicle descends.

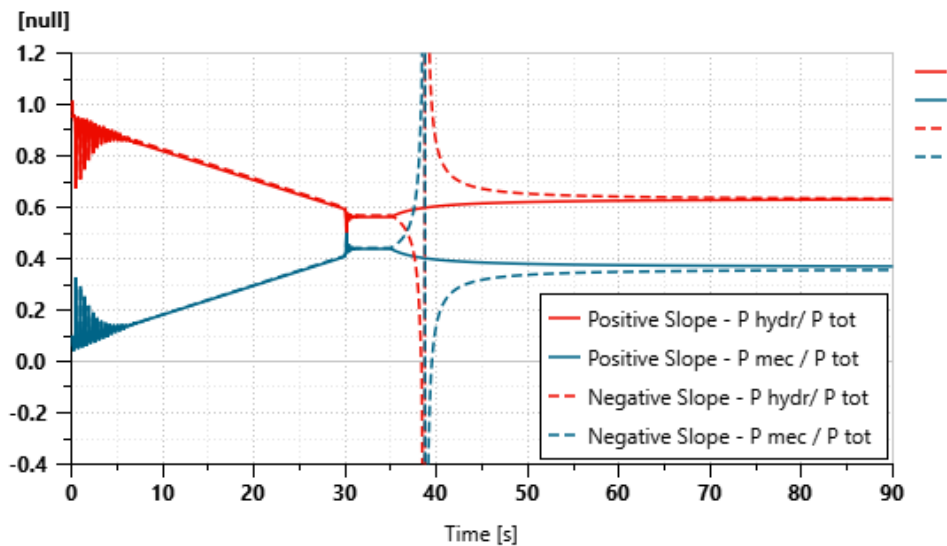


Figure 62: OC low speed \_ Power Ratio

## 7.2.2. High speed

During the high-speed simulations, the transmission behaves differently. As the slope increases, the pressure at the high-pressure line increases, Figure 63, to the point that it reaches 300 bar and the relief valve regulates, from this point, there is a flow rate through the relief valve as

can be seen in Figure 64 and the transmission is not capable of controlling the vehicle's speed causing an increase in the negative slope and a decrease in the positive slope, as shown in Figure 65.

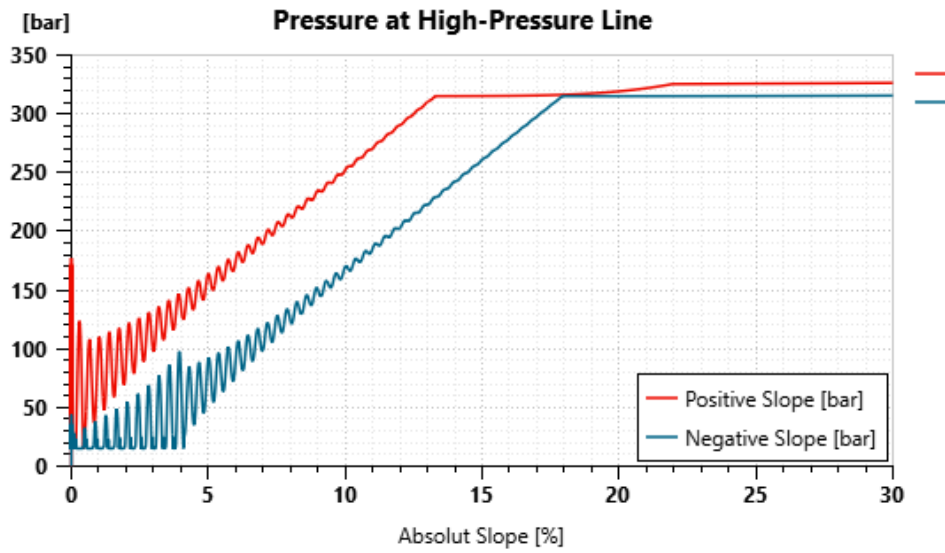


Figure 63: OC high speed \_ pressure at high-pressure line

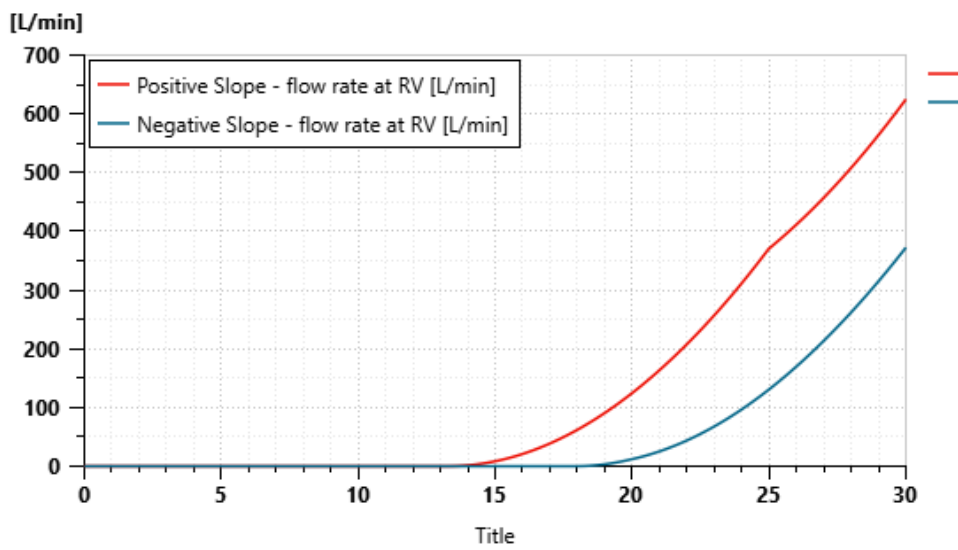


Figure 64: OC high-speed \_flow rate through the relief valve

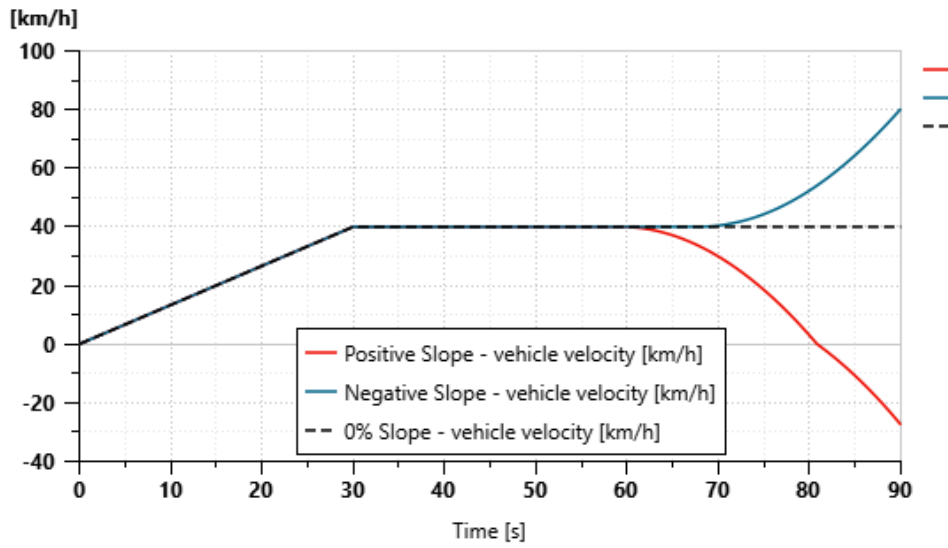


Figure 65: OC high-speed \_ vehicle speed on a slope

In this scenario, all power transmitted in the slope phase is 100% mechanical, whether the vehicle is on a positive or negative slope, as shown in Figure 66.

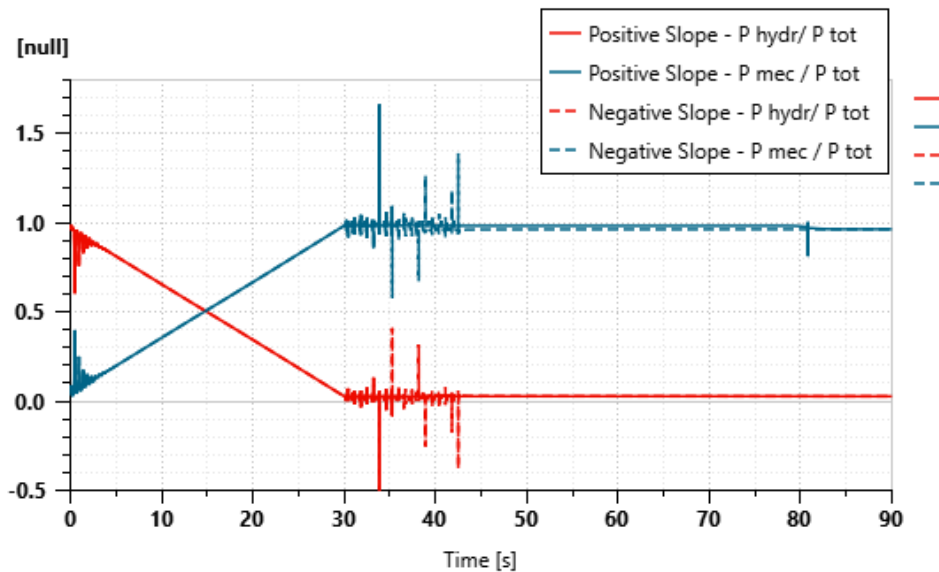


Figure 66: OC high-speed \_ Power Ratio

### 7.3. Input Coupled Results

This section will present the results of the slope simulations for the input-coupled (IC) configuration. Similar to the output-coupled setup, the performance will be assessed for both positive and negative slopes, across low-speed and high-speed scenarios. The discussion will center on vehicle speed, pressure characteristics, and power distribution, with emphasis on the system's behavior under varying slope conditions. These results provide insight into the IC transmission's capacity to manage torque and power flow when subjected to inclines and declines.

### 7.3.1. Low Speed

In the low-speed simulation for the IC configuration on a slope, the vehicle also exhibited a slight increase in speed when subjected to a negative slope and a slight decrease when subjected to a positive slope. As shown in Figure 67, where the dashed black line represents the reference vehicle at 0% slope. No relief valve engagement occurred, as confirmed by the absence of flow through the valve in Figure 68. This indicates that the IC configuration operated within its pressure limits.

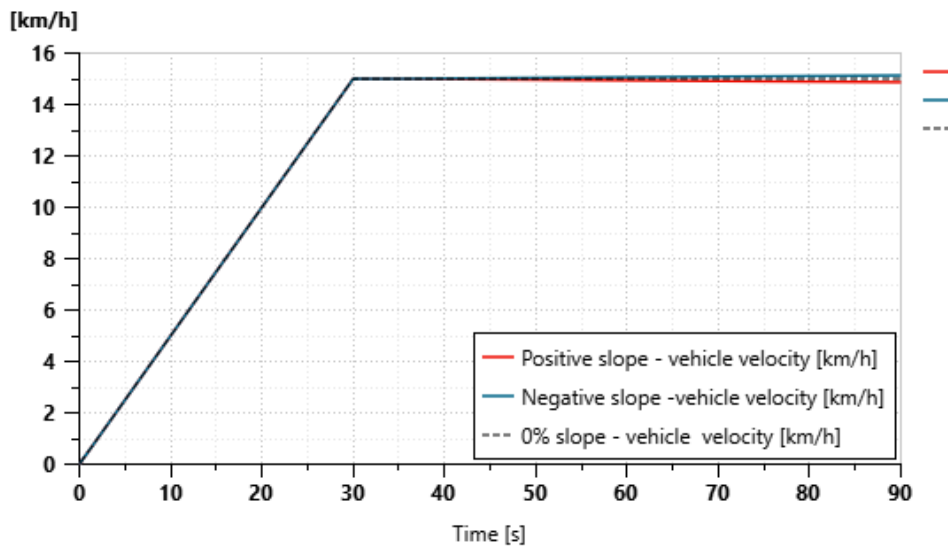


Figure 67: IC low-speed \_ vehicle speed on a slope

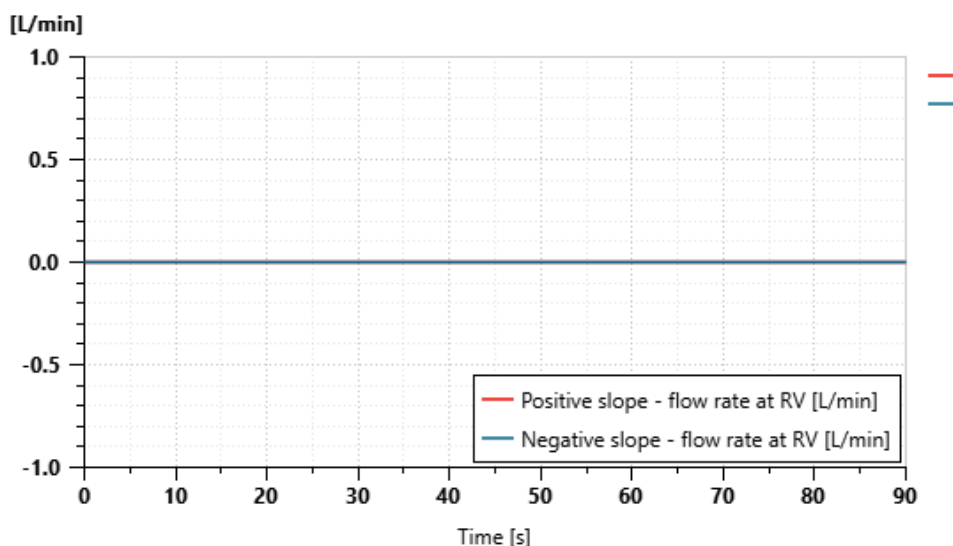


Figure 68: IC low-speed \_flow rate through the relief valve

As mentioned before in the section 7.2, the vehicle is submitted to a positive torque in a positive slope and to a negative torque in a negative slope. Similar to the OC scenario, IC configuration also inverts the high and low-pressure lines, as illustrated in Figure 69.

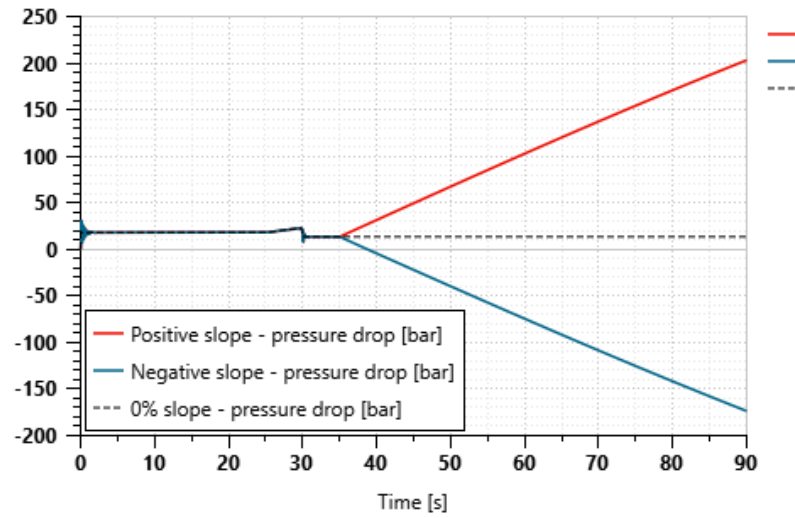


Figure 69: IC low speed \_ pressure drop between high and low-pressure lines

Figure 70 presents the power ratio for both positive and negative slope scenarios. In this case, the transmission appears to respond in the same way for both slope scenarios.

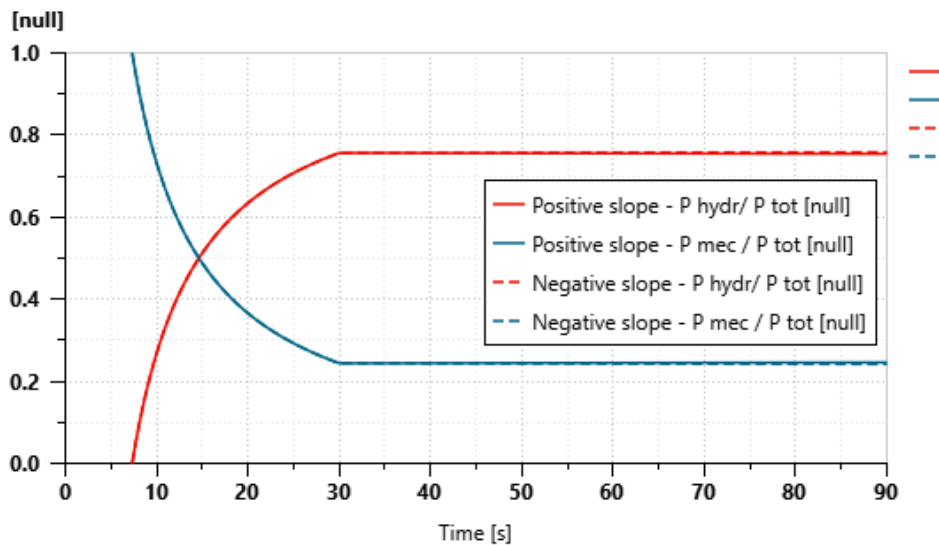


Figure 70: IC low speed \_ Power Ratio

### 7.3.2. High Speed

At higher speeds, the IC configuration shows more noticeable effects under varying slope conditions. The pressure at the high-pressure line increases significantly as the vehicle faces a steeper slope, as seen in Figure 71. Once the pressure reaches the relief valve threshold (300 bar), the valve opens, as indicated by the flow rate in Figure 72. This results in the system losing speed control, with vehicle speed decreasing on positive slopes and increasing on negative slopes, as shown in Figure 73.

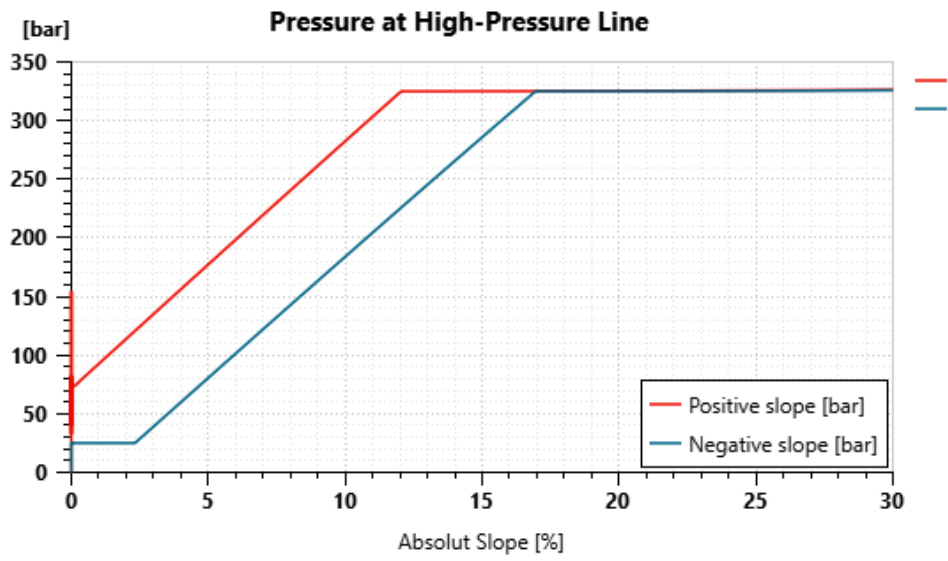


Figure 71: IC high speed \_ pressure at high pressure-line

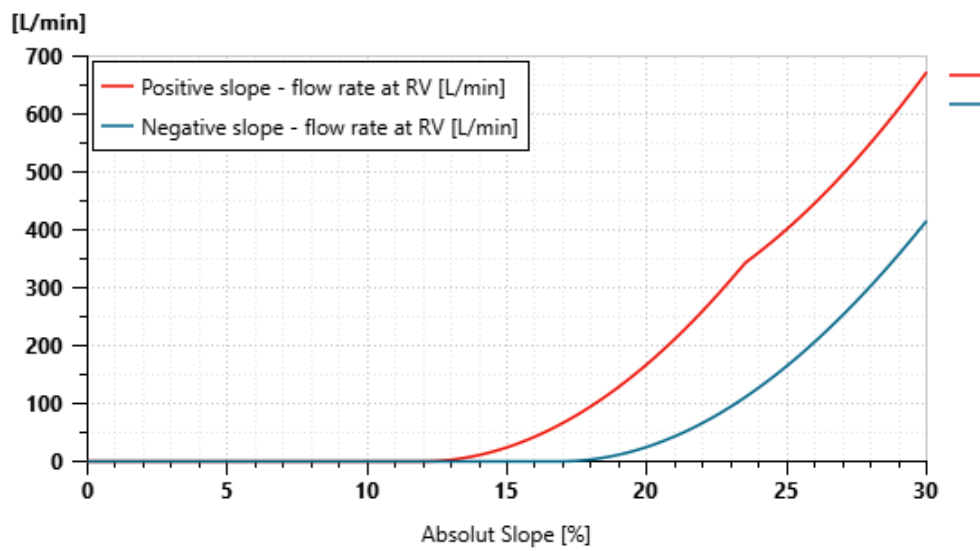


Figure 72: IC high speed \_ flow rate through the relief valve

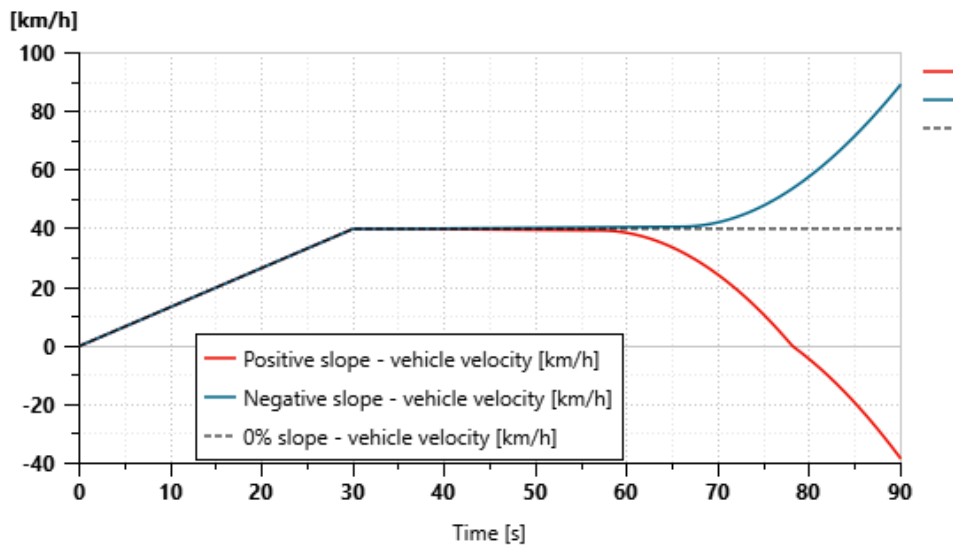


Figure 73: IC high speed \_ vehicle speed on a slope

In this scenario, opposite to the result obtained in the OC case, the power transmitted is majorly hydrostatic, as can be observed in Figure 74.

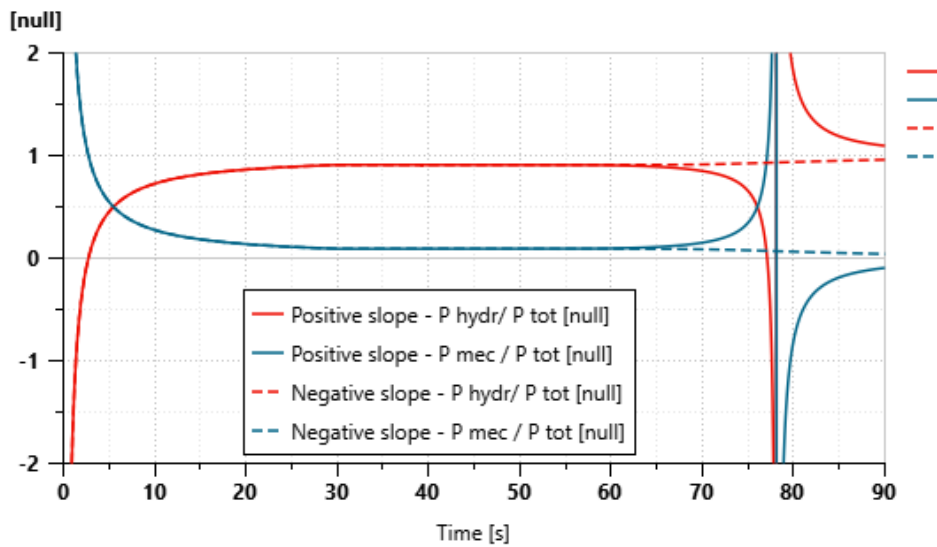


Figure 74: IC high speed \_ Power Ratio

## Chapter 8. Analysis of Input Coupled Configuration

In this chapter, the influence of several key parameters on the Input-Coupled (IC) configuration is analyzed. These parameters include the displacement of both the primary ( $V_I$ ) and secondary ( $V_{II}$ ) hydraulic units, the transmission ratio ( $i_1$ ) between the internal combustion engine (ICE) and hydraulic unit (HU), the transmission ratio ( $i_2$ ) between the hydraulic unit and planetary gear, and the ring-to-sun ratio ( $\tau_0$ ) in the planetary gear system. The analysis focuses on how these changes affect vehicle speed, power distribution between mechanical and hydraulic paths, and the behavior of the relief valve under different conditions.

The simulations were performed as *batch runs* for each parameter to be analyzed, with a 50-second duration. Two scenarios were evaluated, in the first scenario the speed of the vehicle was increased from 0 to 40 *km/h* in constant acceleration, as shown in Figure 75 as the red line (Scenario 1), with a maximum torque of 4946 *Nm*. In the other scenario, the speed profile requested for the vehicle is shown in Figure 75 as the blue line (Scenario 2) where the speed increases from 0 to 100 *km/h*, with a maximum torque of 9376 *Nm*. Each parameter was changed separately while the other parameters remained as the reference values shown in Table 5.

Table 5: Reference values for a batch run

Reference Values	
$V_I$	$80\text{cm}^3/\text{rev}$
$V_{II}$	$80\text{cm}^3/\text{rev}$
$i_1$	1.77
$i_2$	3.6
$\tau_0$	-5.0

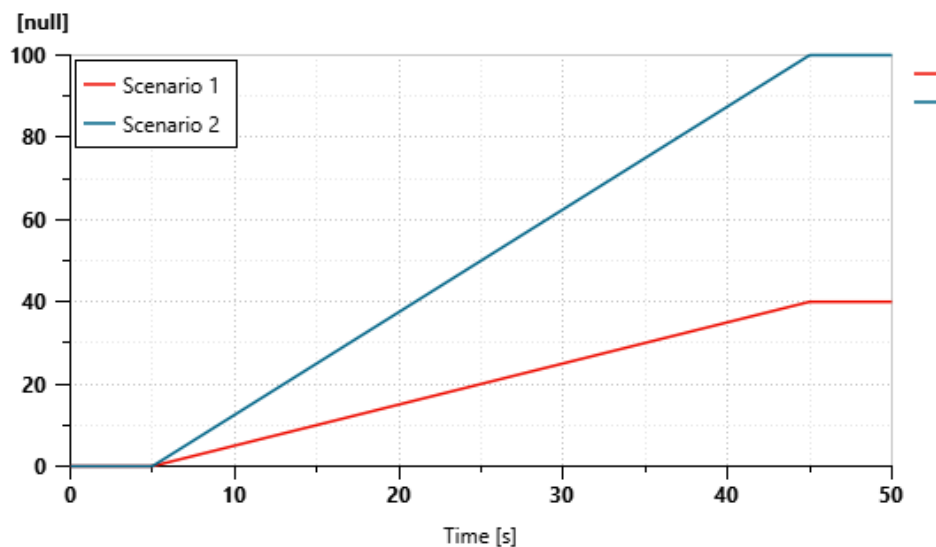


Figure 75: Requested speed profile

## 8.1. Effect of Primary Unit Displacement

For the analysis of the effect of primary unit displacement, batch simulations were conducted with varying maximum displacements of the primary hydraulic unit. The baseline displacement was set at  $80 \text{ cm}^3/\text{rev}$ , and five simulations were performed with values of 40, 80, 120, 160, and  $200 \text{ cm}^3/\text{rev}$ .

Figure 76 shows the displacement control to achieve scenario 1's speed profile. As can be observed, the smaller the maximum displacement of the primary unit, the steeper the solid line, which represents the percentage of the primary unit displacement. Since all scenarios have the same shaft speed for the primary unit, smaller pumps require a larger percentage of their total displacement to produce the necessary flow rate, while larger pumps can achieve the same flow with a lower displacement percentage.

The red line in Figure 76, which represents the smallest pump, shows a limitation in achieving the target speed, leading to a discontinuity in the dashed red line. This indicates that the control system is struggling to meet the demand due to the pump's limited displacement capacity. The impact of this is evident in Figure 77, where the vehicle's speed begins to decline around 38 seconds, highlighting that the smaller pump cannot maintain the required flow rate to sustain the target speed under the given conditions.

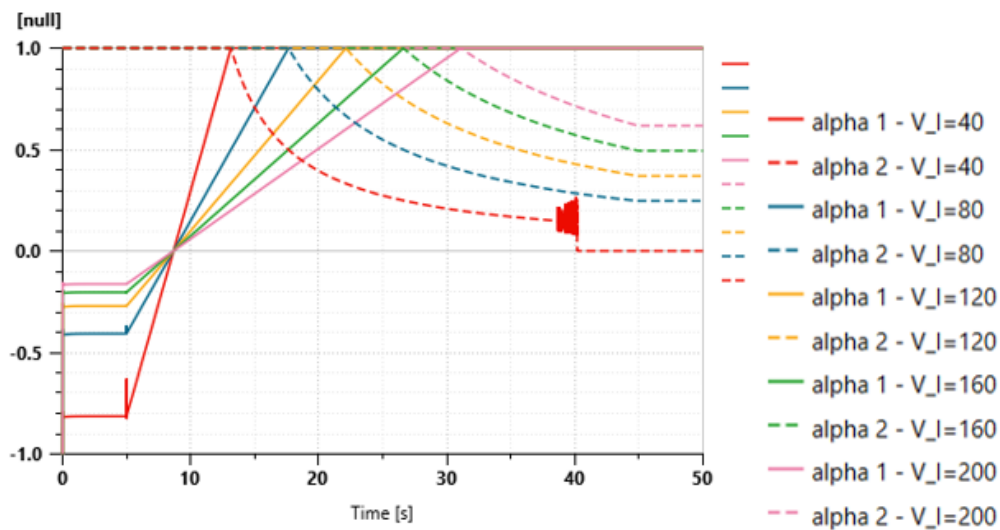


Figure 76: Displacement control

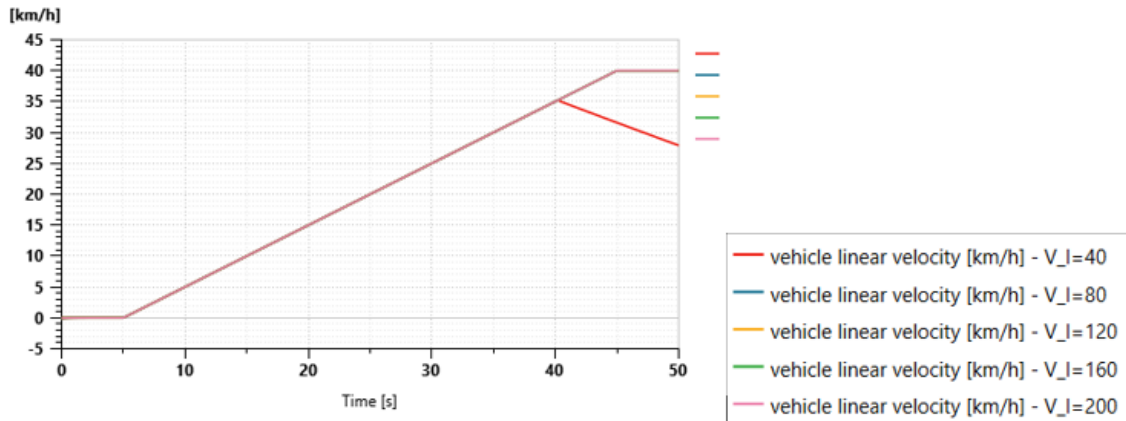


Figure 77: Vehicle speed

Figure 78 shows the pressure drop between the high-pressure line and the low-pressure line. The torque required is the same in every case a higher pressure drop is necessary to generate the same torque at the secondary unit's shaft when using a smaller displacement. This relationship is evident when comparing the secondary unit's displacement (dashed line) in Figure 76 with the pressure drop in Figure 78, where the same vehicle configuration is represented by the same colors. This also explains why the 40  $cm^3/rev$  case fails to reach the target speed due to relief valve regulation, as shown by the flow rate through the relief valve in Figure 79.

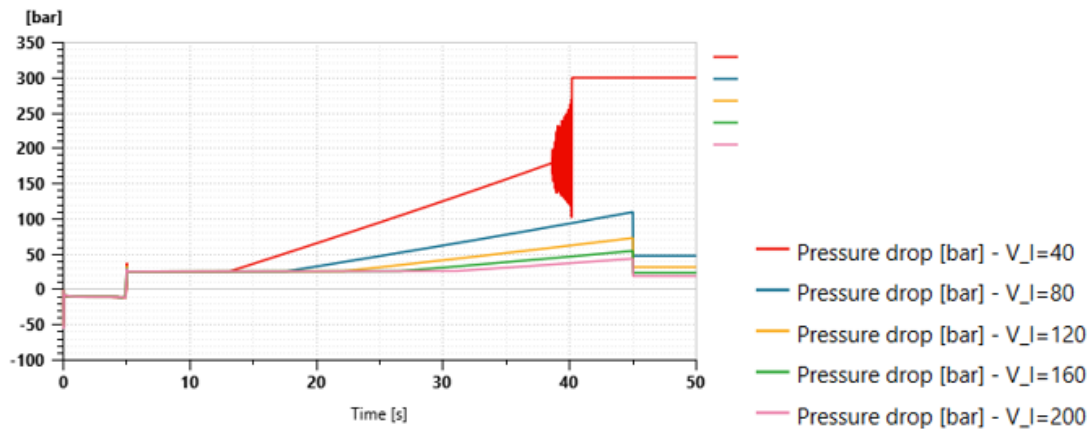


Figure 78: Pressure drop between high and low-pressure lines

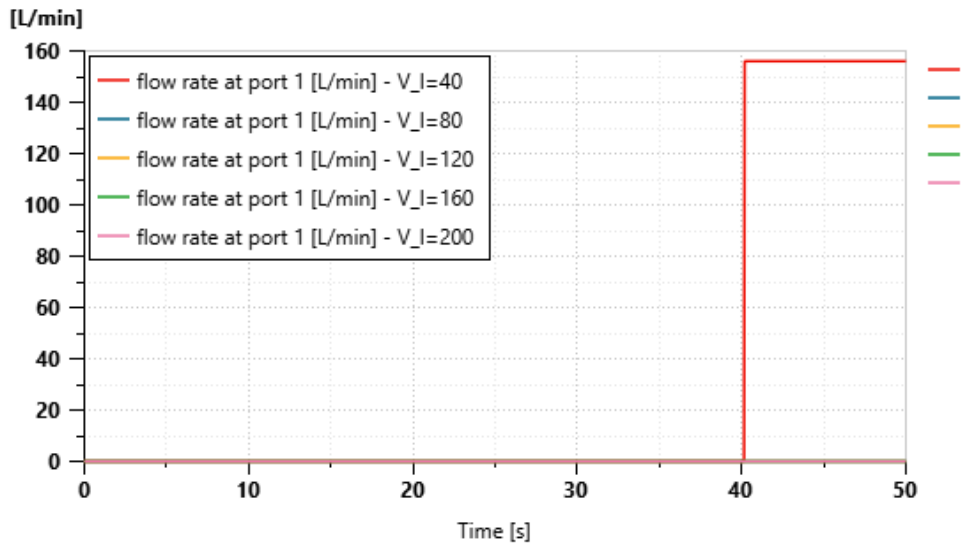


Figure 79: Flow rate through the relief valve

Furthermore, changing the maximum displacement of the primary unit doesn't change the power distribution between hydraulic and mechanical path, as shown in Figure 80.

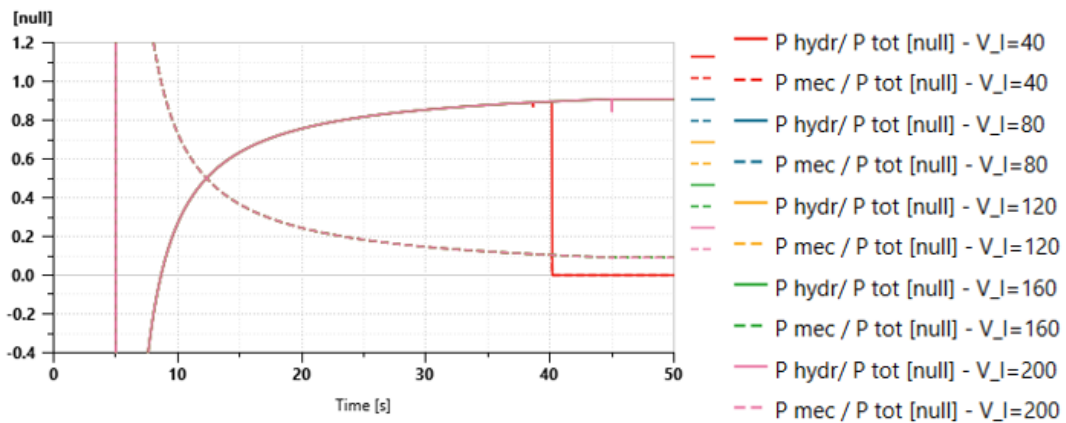


Figure 80: Power ratio

The vehicle's speed achieved in scenario 2 for each case is shown in Figure 81, as expected, the smaller the maximum displacement of the primary unit, the smaller the maximum speed achieved, due to the higher pressure drop and the regulation of the relief valve as explained before. It is also important to highlight that in this scenario, the torque requested is higher which explains the smaller maximum speed achieved by the  $40 \text{ cm}^3/\text{rev}$  pump.

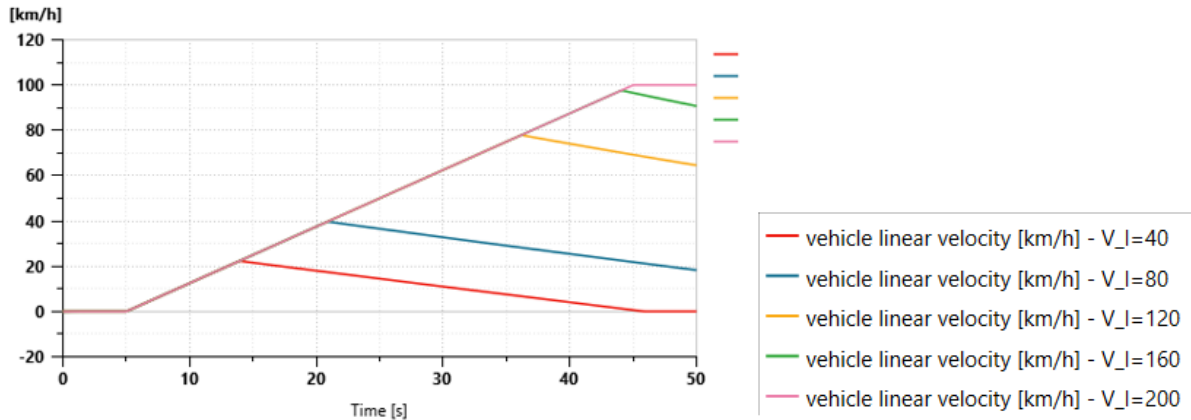


Figure 81: Scenario 2 - Vehicle speed

## 8.2. Effect of Secondary Unit Displacement

To assess the effect of secondary unit displacement on the system's performance, a series of batch simulations were conducted. These simulations were set up similarly to the primary unit analysis, with a reference value for displacement at  $80 \text{ cm}^3/\text{rev}$ . Simulations were carried out with values of 40, 80, 120, 160, and  $200 \text{ cm}^3/\text{rev}$ , allowing for a comparison of how varying secondary unit displacement impacts the vehicle's performance.

Figure 82 shows the displacement control to achieve scenario 1's speed profile. In an ideal hydrostatic transmission, all the flow rate generated by the primary unit is directly transferred to the secondary unit. At the beginning of the mission, the secondary unit is at its maximum displacement, therefore, a smaller secondary unit requires a smaller percentage of the primary unit's displacement to generate the same shaft speed, explaining why the solid lines are steeper for greater secondary units. When the primary unit reaches its maximum displacement, the displacement of the secondary unit has to be the same in all cases since the flow rate and the shaft speed are the same, explaining the faster decrease in the secondary unit's displacement for the bigger units.

In this case, all the displacements tested achieved the speed profile requested, as can be seen in Figure 83. Therefore, the relief valve doesn't regulate in any of the cases, as shown in Figure 84, there is no flow rate through the valve.

Following the same logic, to generate the same torque a smaller displacement requires a greater pressure drop, as can be observed in Figure 85. When the displacement is equal, the pressure drop is also the same.

Adjusting the secondary unit's maximum displacement does not affect the distribution of power between the hydraulic and mechanical paths, as illustrated in Figure 86.

The vehicle's speed achieved in scenario 2 for each case is shown in Figure 87. A smaller maximum displacement in the secondary unit allows for higher rotational speeds to achieve the necessary flow rate for a given speed profile. Since the unit delivers a lower volume per revolution, it needs to spin faster to match the system's flow requirements. This increase in

rotational speed enables the vehicle to reach higher speeds while maintaining the flow balance between the primary and secondary units. Consequently, the vehicle achieves a greater maximum speed when the secondary unit displacement is minimized.

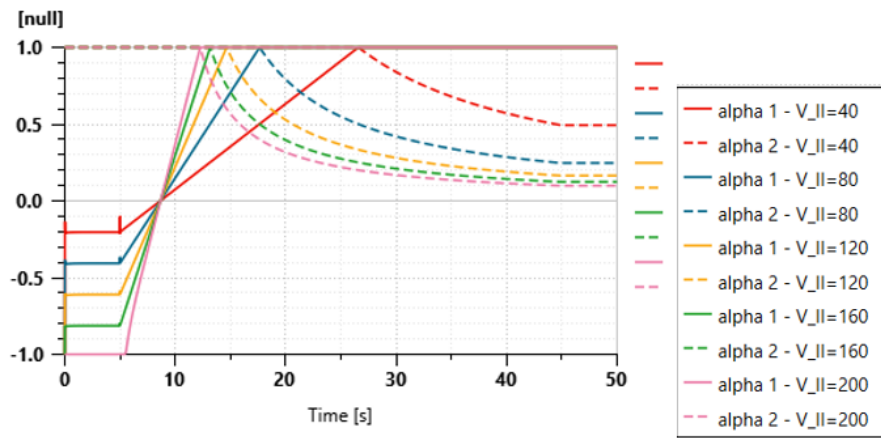


Figure 82: Displacement control

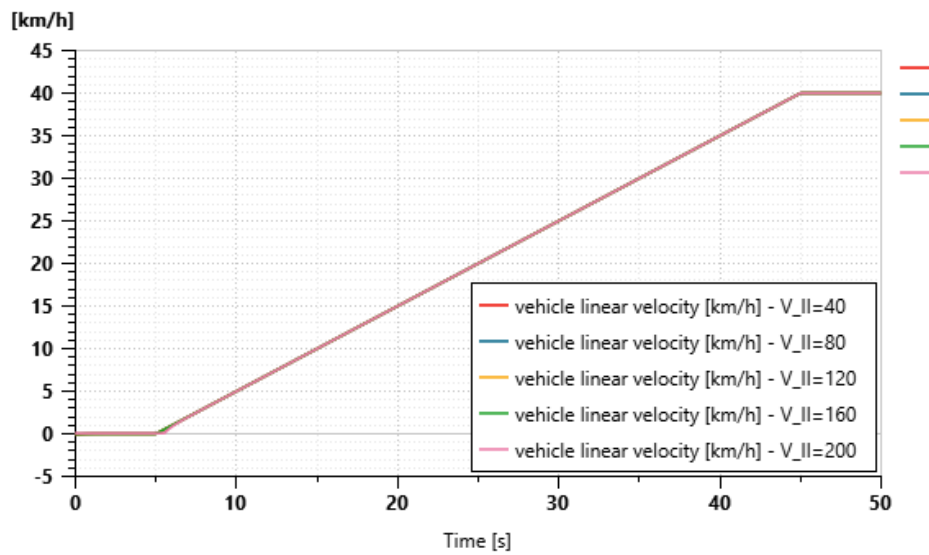


Figure 83: Vehicle speed

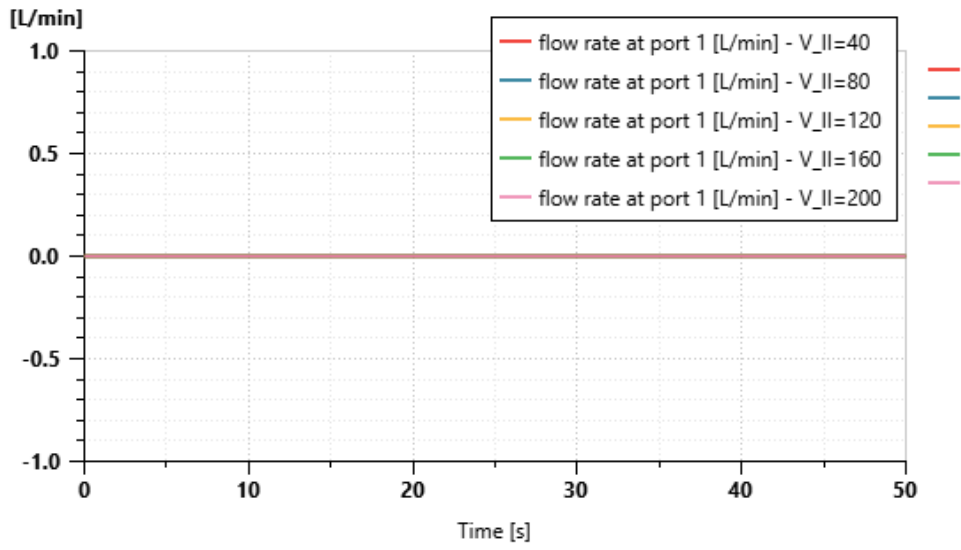


Figure 84: Flow rate through the relief valve

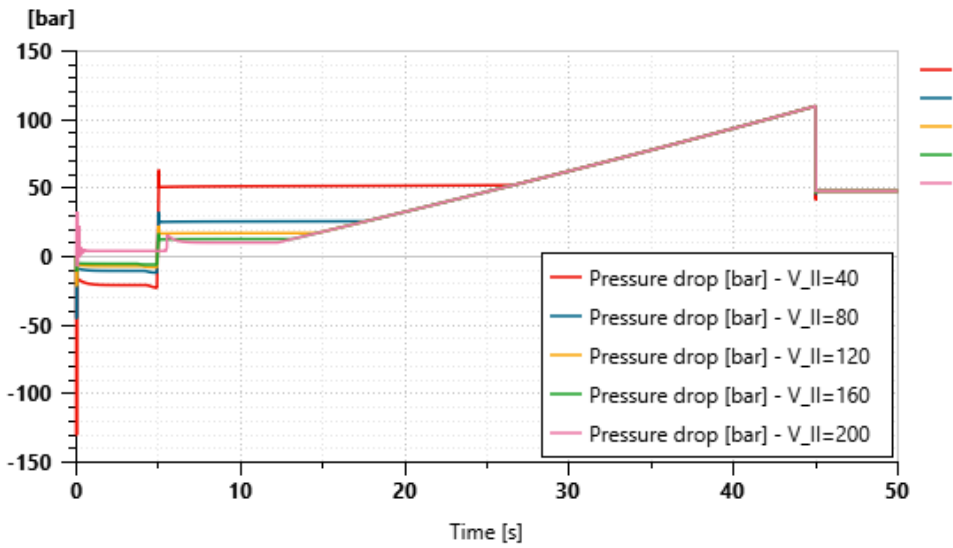


Figure 85: Pressure drop between high and low-pressure lines

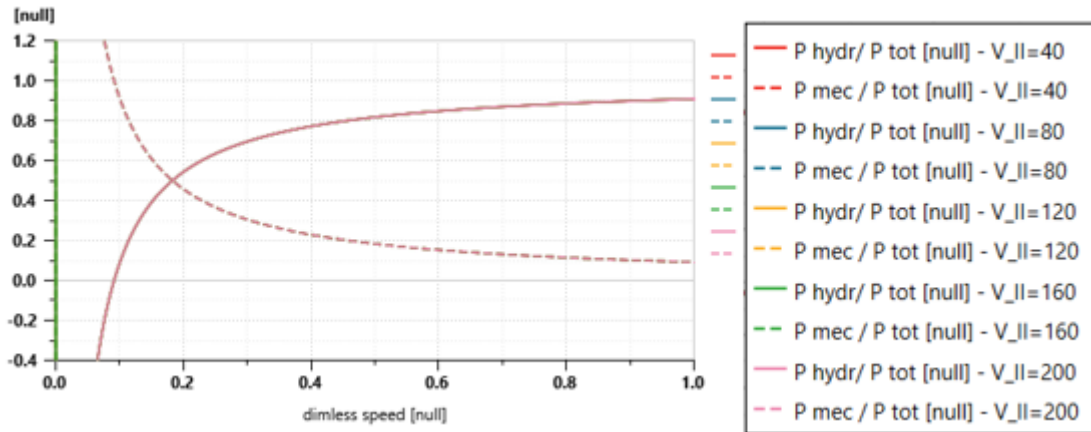


Figure 86: Power ratio

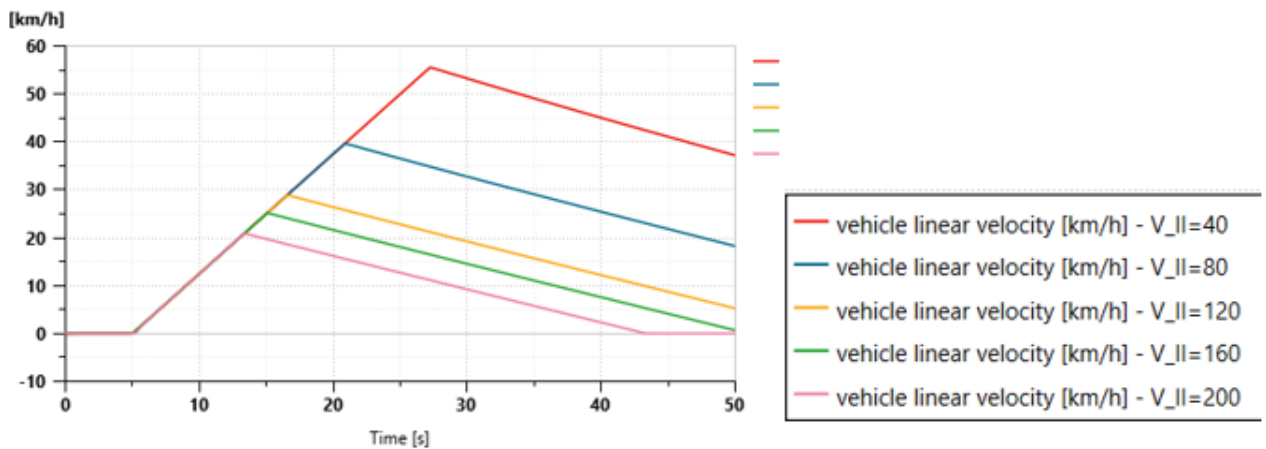


Figure 87: Scenario 2 - Vehicle speed

### 8.3. Effect of Transmission Ratio Between Prime Mover and Primary Hydraulic Unit ( $i_1$ )

For the analysis of the effect of the transmission ratio between the prime mover and the primary hydraulic unit, batch simulations were conducted in which the transmission ratios analyzed were 1.13, 1.29, 1.45, 1.61, and 1.77. These ratios modify the relationship between engine speed and the hydraulic primary unit's shaft speed, influencing both the flow rate and the vehicle's speed response.

Figure 88 illustrates how different transmission ratios influence the displacement control required to achieve Scenario 1's speed profile. With higher transmission ratios, less displacement percentage from the primary unit is needed to reach the same flow rate, since the increase of the transmission ratio results in a higher input shaft's speed. Lower ratios, by contrast, demand higher displacement percentages to maintain the target speed, as shown by the steeper increase in displacement requirements. All the transmission ratios analyzed here were capable of achieving the requested speed profile, as shown in Figure 89.

In terms of relief valve engagement, Figure 90 indicates that higher transmission ratios help maintain pressure within acceptable limits, as they reduce the need for high displacement

values. In the cases simulated there was regulation of the relief valve as can be seen in Figure 91 there is no flow rate through the valve.

For the load and the speed profile requested for scenario 1, the change in the transmission ratio doesn't influence the power distribution between hydrostatic and mechanical power, as illustrated in Figure 92.

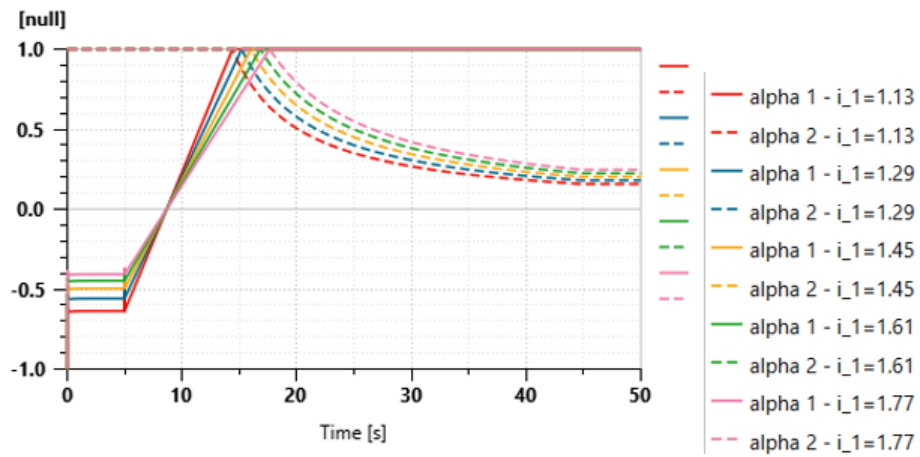


Figure 88: Displacement control

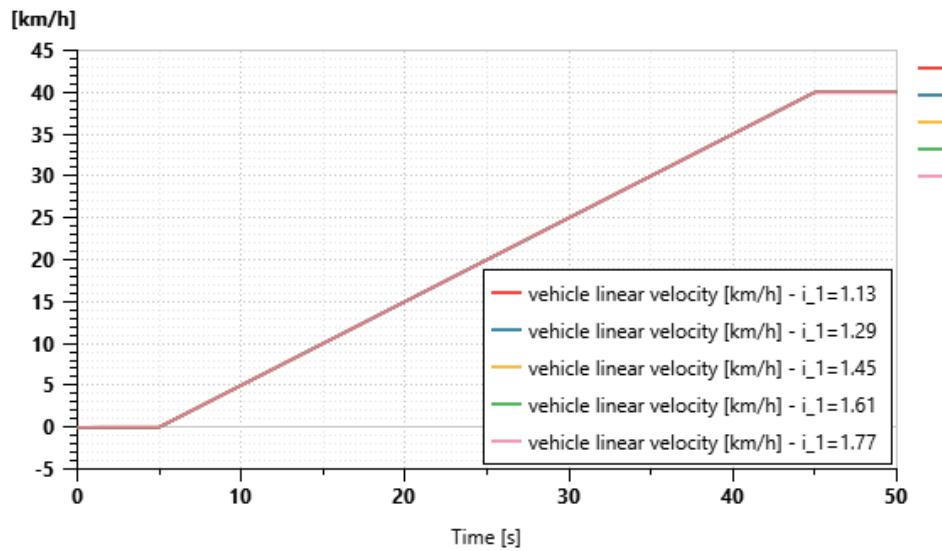


Figure 89: Vehicle speed

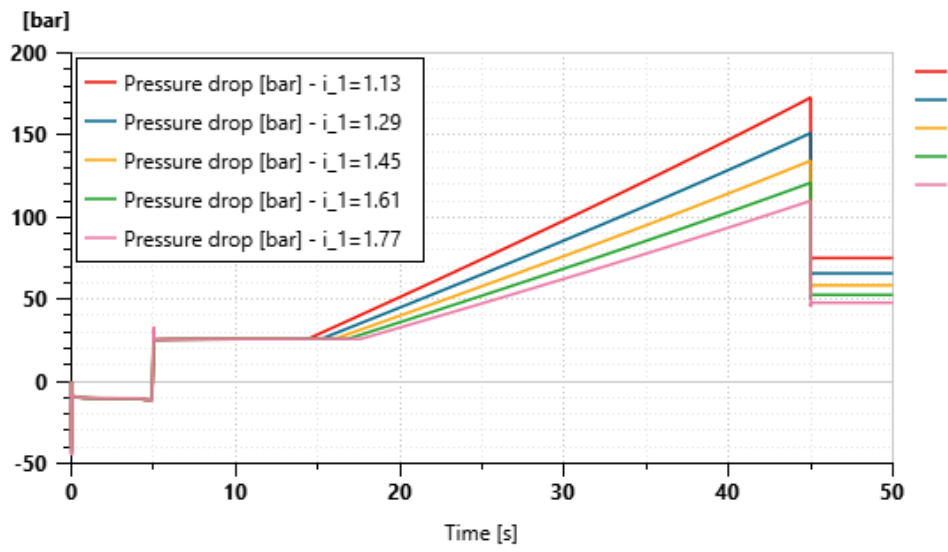


Figure 90: Pressure drop between high and low-pressure lines

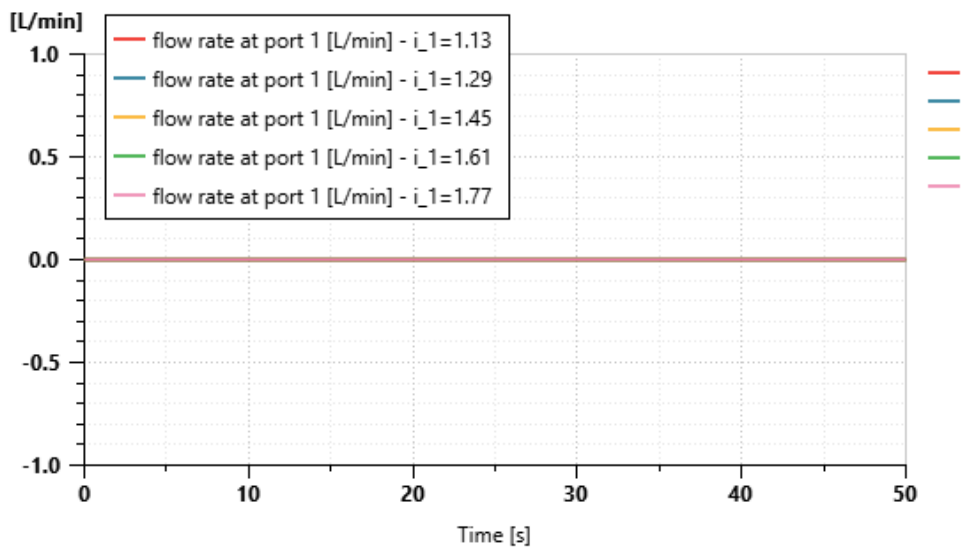


Figure 91: Flow rate through the relief valve

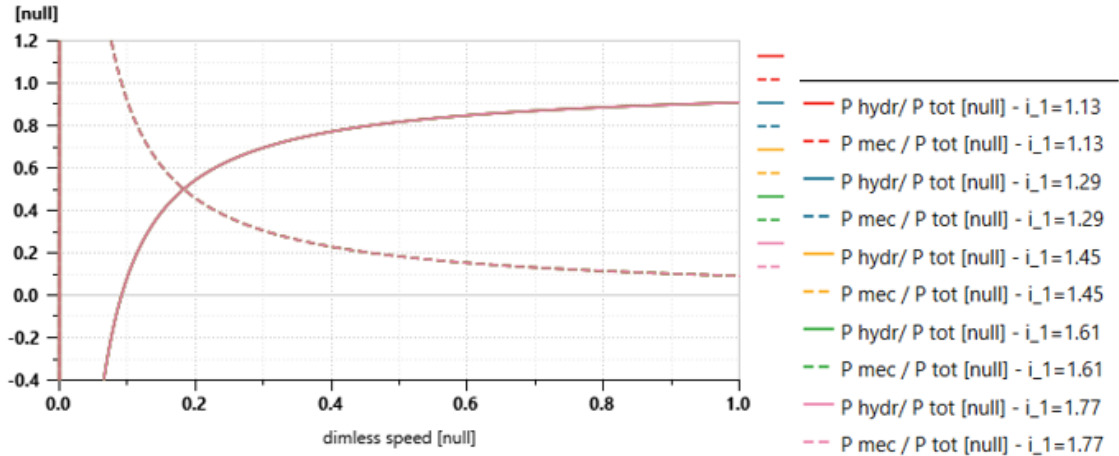


Figure 92: Power ratio

## 8.4. Effect of Transmission Ratio Between HU and Planetary Gear ( $i_2$ )

For analyzing the impact of the transmission ratio between the hydraulic unit (HU) and the planetary gear on performance, batch simulations were conducted with ratios of 1.6, 2.1, 2.6, 3.1, and 3.6. This adjustment changes the speed relationship between the HU and the planetary gear.

Figure 93 shows the displacement control necessary to achieve scenario 1's speed profile. The percentage of displacement in the primary and secondary units varies across the transmission ratios. Lower ratios, such as 1.6 and 2.1, required a higher displacement percentage initially to meet the flow demand, while higher ratios achieved the target flow more rapidly, reducing the displacement percentage required throughout the mission. In this scenario, the transmission was able to complete the mission in all cases, as can be seen in Figure 94.

Figure 95 illustrates the pressure drop across the hydraulic system for each transmission ratio. Across all ratios, the pressure drop remains below the maximum pressure allowed for the system, which means that the relief valve doesn't regulate, as can be seen in Figure 96, there is no flow rate through it. Furthermore, higher ratios experience a slightly reduced pressure drop. This reduction occurs because the increased rotational speed at higher ratios allows the system to manage pressure more efficiently while producing the required torque. The trade-off here is that while lower ratios are more effective at maintaining torque at lower speeds, higher ratios can handle pressure more efficiently at higher speeds. This explains why the case with the transmission ratio of 3.6 reaches a smaller maximum speed in scenario 2, as illustrated in Figure 98.

For the load and speed profile of scenario 1, the variation in the transmission ratio does not affect the power distribution between hydrostatic and mechanical power, as shown in Figure 97.

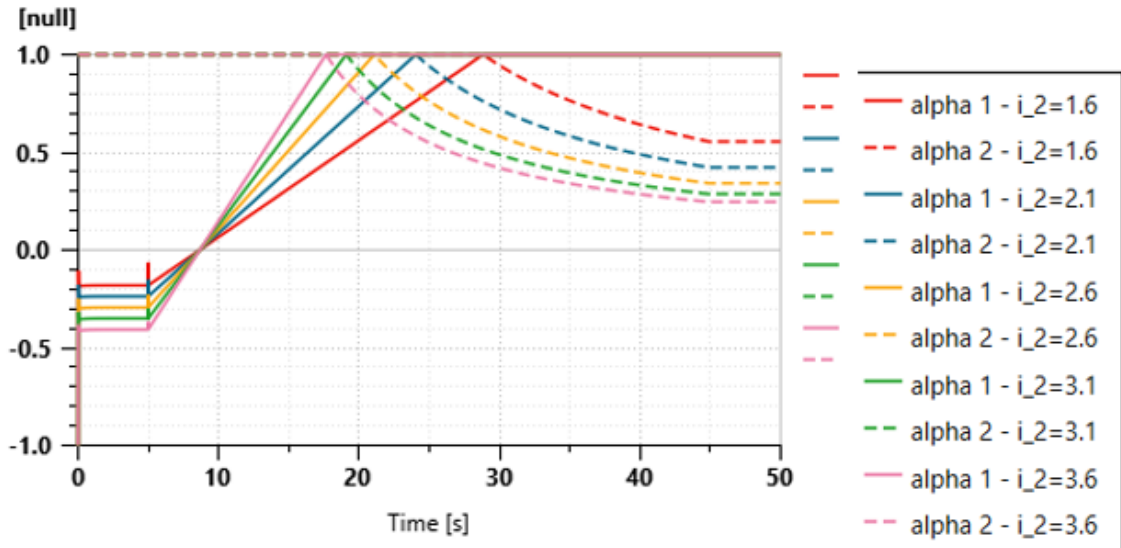


Figure 93: Displacement control

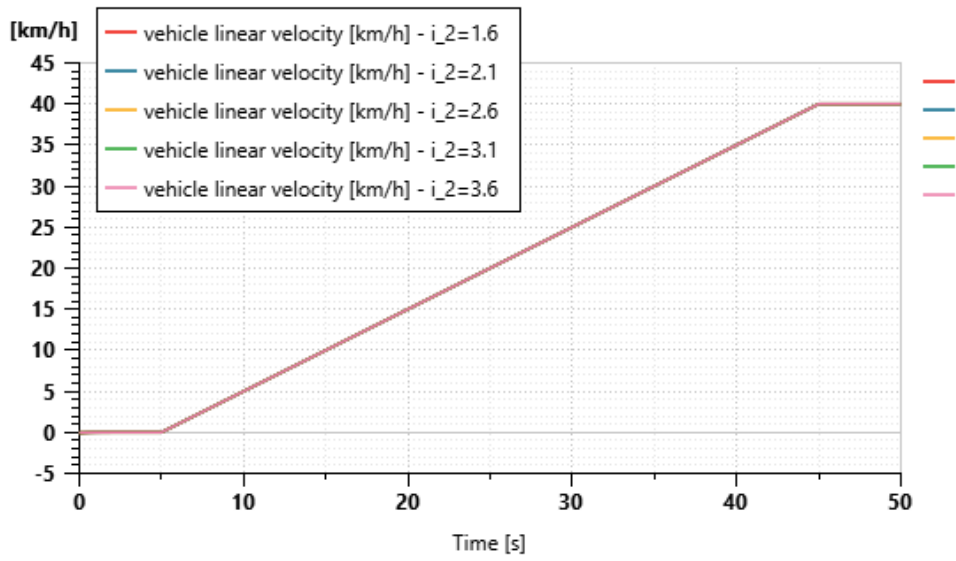


Figure 94: Vehicle speed

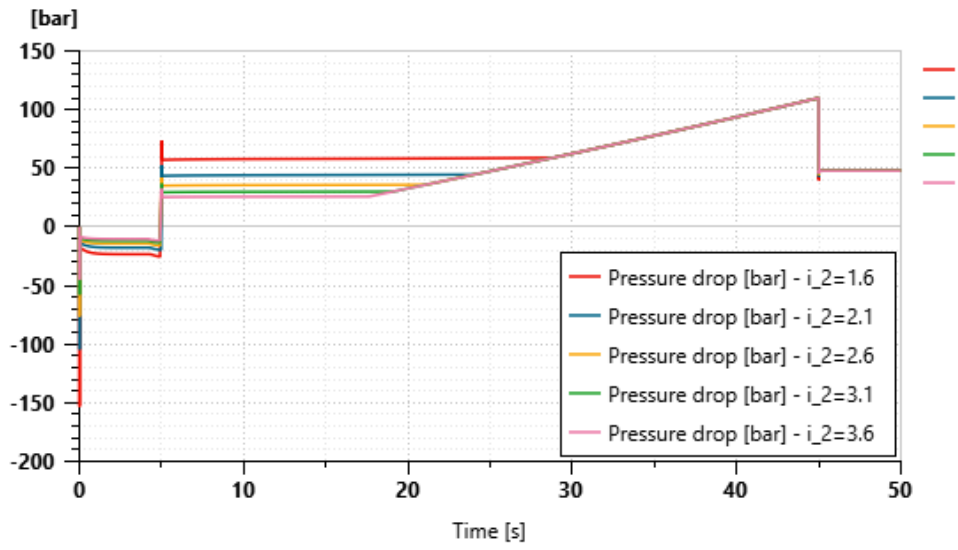


Figure 95: Pressure drop between high and low-pressure lines

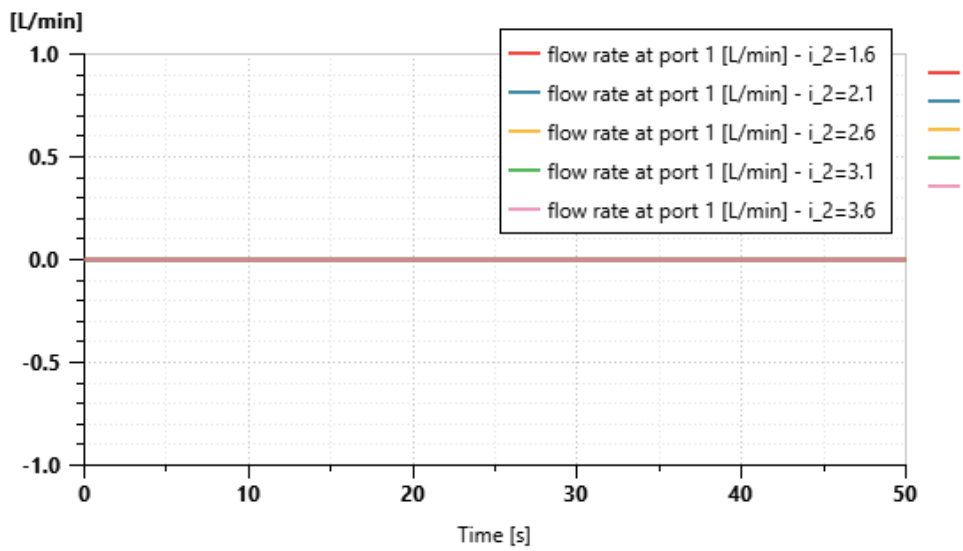


Figure 96: Flow rate through the relief valve

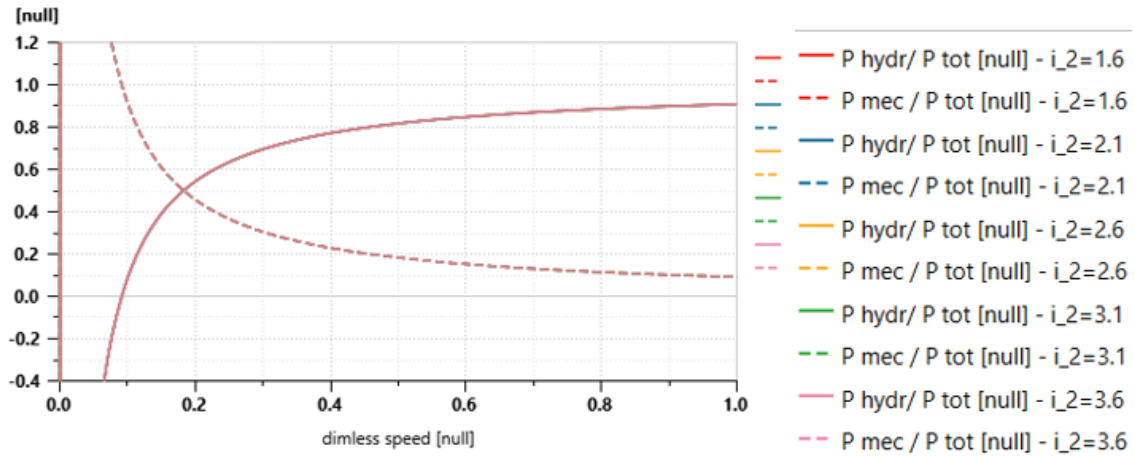


Figure 97: Power ratio

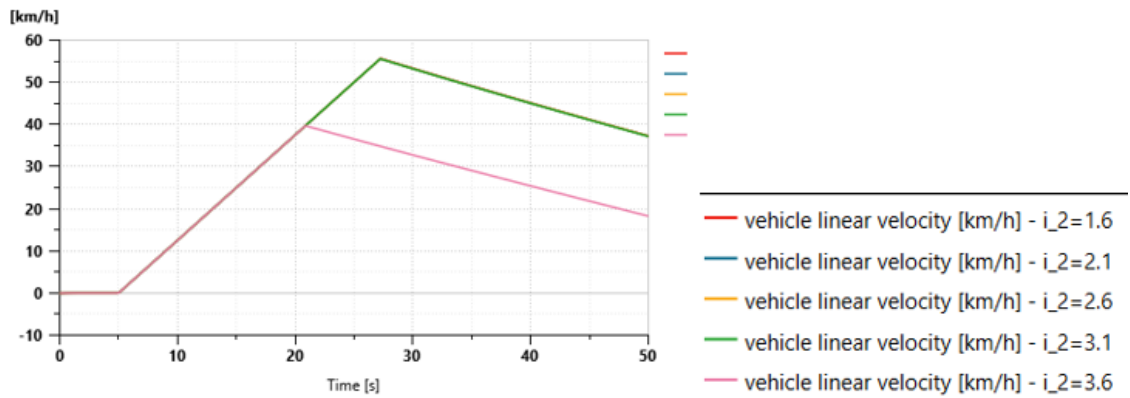


Figure 98: Scenario 2 - Vehicle speed

## 8.5. Effect of Planetary Gear Transmission Ratio ( $\tau_0$ )

To analyze the effect of the planetary gear transmission ratio on system performance, batch simulations were conducted using ratios of  $-5.0$ ,  $-4.3$ ,  $-3.6$ ,  $-2.9$ , and  $-2.2$ . This variation in ratios modifies the speed relationship between the planetary gear and the overall system.

Figure 99 illustrates the displacement control required to achieve the desired speed profile in scenario 1. The percentage of displacement in both the primary and secondary units changes with different planetary gear transmission ratios. Lower negative ratios, such as  $-2.2$  and  $-2.9$ , necessitated a greater displacement percentage initially to meet the flow demands. In contrast, higher ratios (closer to  $-5.0$ ) were able to reach the target flow more efficiently, thus requiring a reduced displacement percentage throughout the operation. The system successfully completed the mission across all ratios, as demonstrated in Figure 100.

Figure 101 shows the pressure drop across the hydraulic system for each planetary gear transmission ratio. Throughout the range of ratios, the pressure drop remained within acceptable limits, indicating effective management of hydraulic pressure throughout the simulation. Lower ratios tended to exhibit a slight reduction in pressure drop, attributed to improved efficiency in managing pressure and torque at elevated speeds. Figure 102 further

illustrates that the relief valve did not activate across these ratios, as there was no flow rate through the valve.

In this scenario, lower planetary gear transmission ratios ( $\tau_0$ ) demonstrated a smoother transition between the percentages of mechanical power and hydrostatic power, as illustrated in Figure 103. These lower ratios resulted in a greater percentage of mechanical power at higher speeds, which is particularly beneficial in high-torque applications.

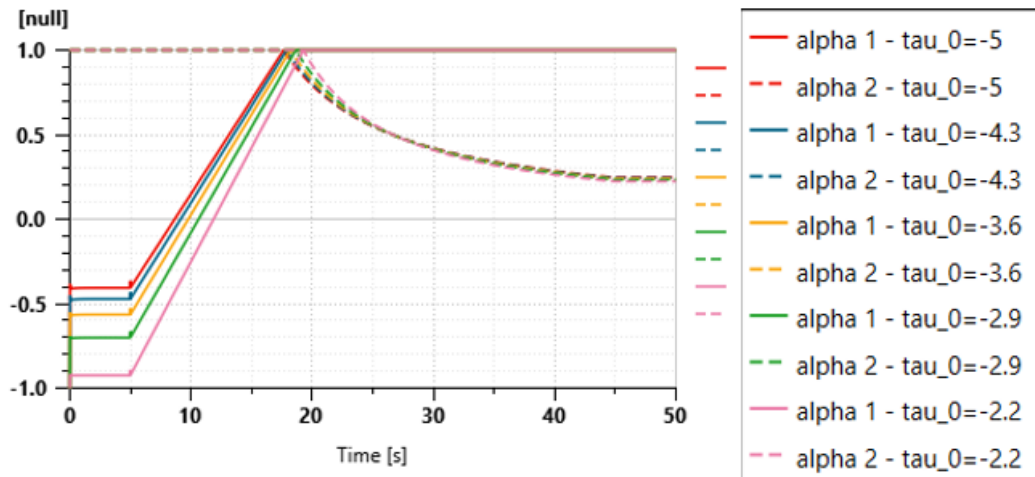


Figure 99: Displacement control

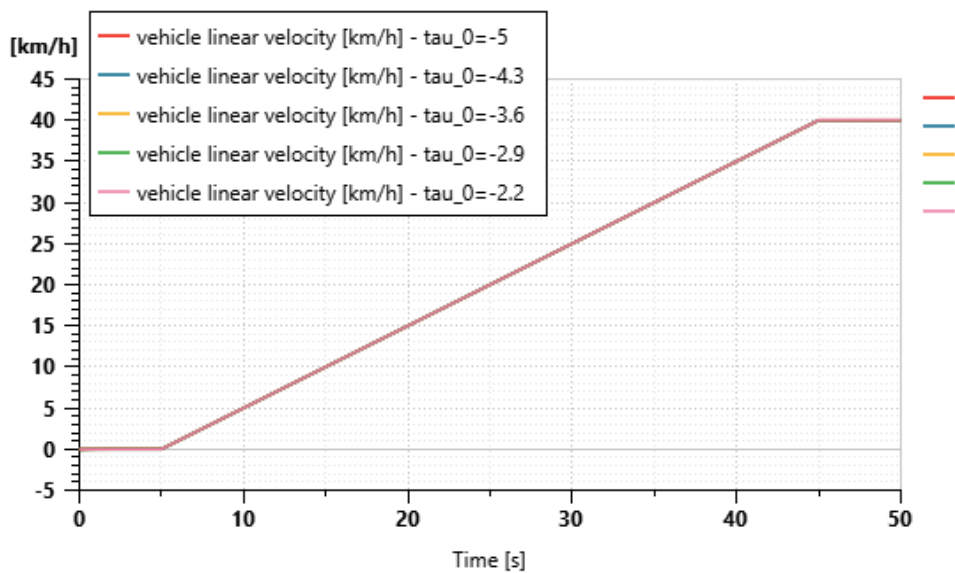


Figure 100: Vehicle speed

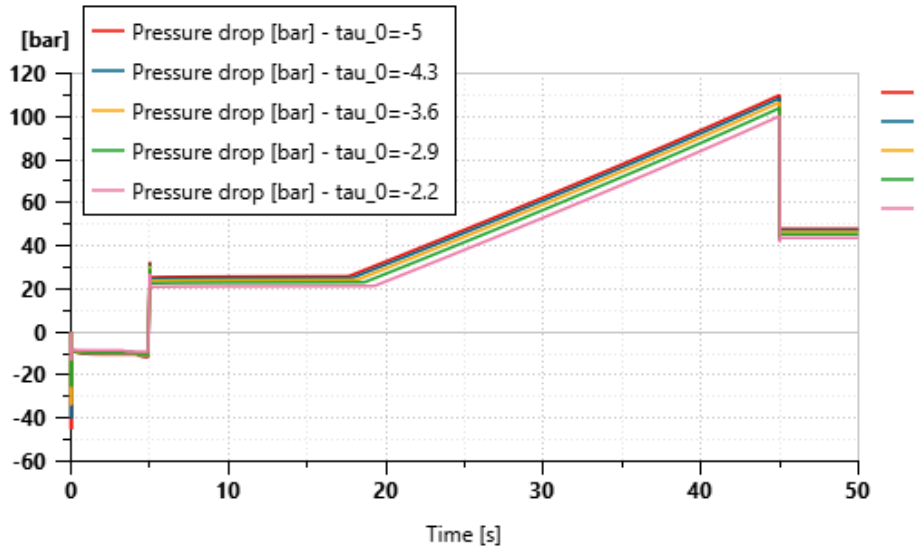


Figure 101: Pressure drop between high and low-pressure lines

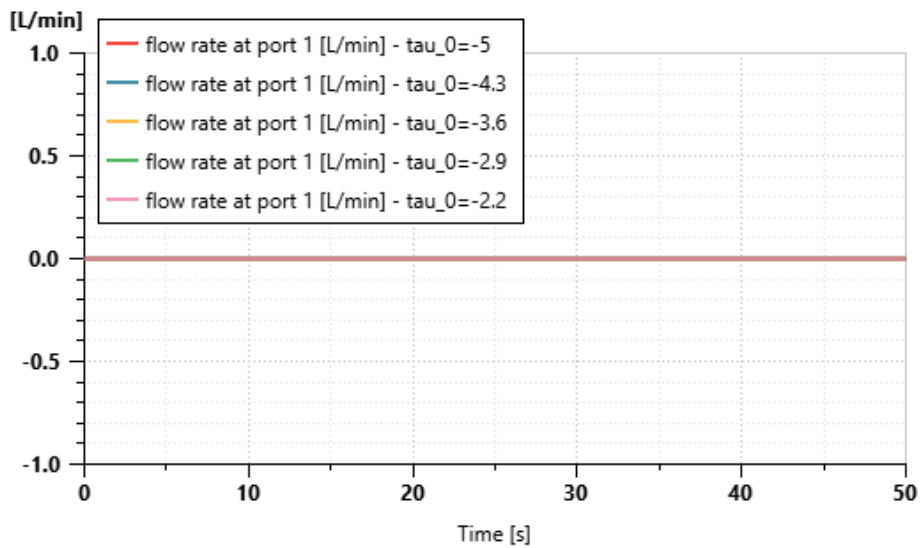


Figure 102: Flow rate through the relief valve

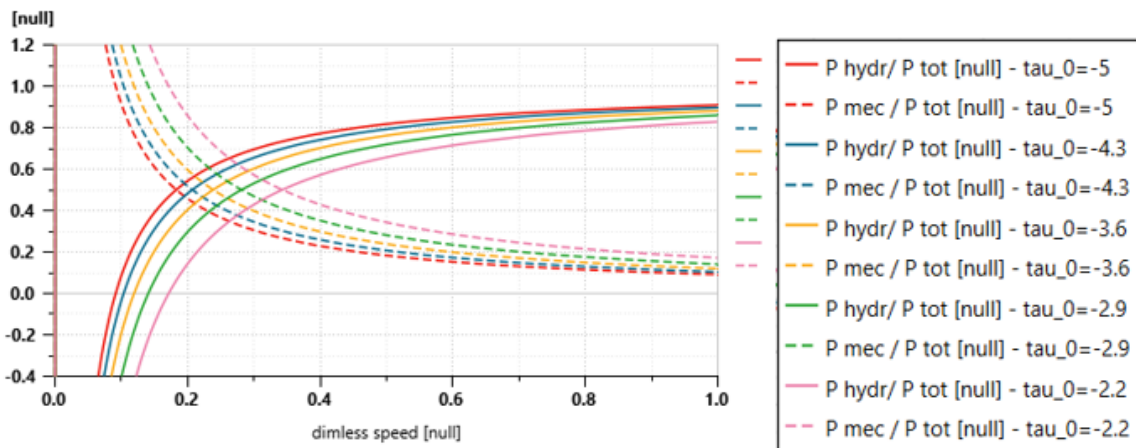


Figure 103: Power ratio

## Chapter 9. Conclusion

This thesis analyzed the performance of hydromechanical transmissions, focusing on input-coupled (IC) and output-coupled (OC) configurations. Through Simcenter Amesim simulations, the study examined power and torque distribution, speed response, and slope performance to understand how each configuration meets varying operational demands.

The OC configuration demonstrated a smooth transition from hydrostatic to mechanical torque as speed increased, favoring mechanical power at higher speeds. Conversely, the IC configuration showed a strong reliance on hydrostatic power at low speeds, providing responsive acceleration but requiring careful management to optimize performance over time. Under PID control, both configurations successfully followed speed profiles, though with unique power distribution patterns that highlighted the impact of configuration choice on power management and control dynamics.

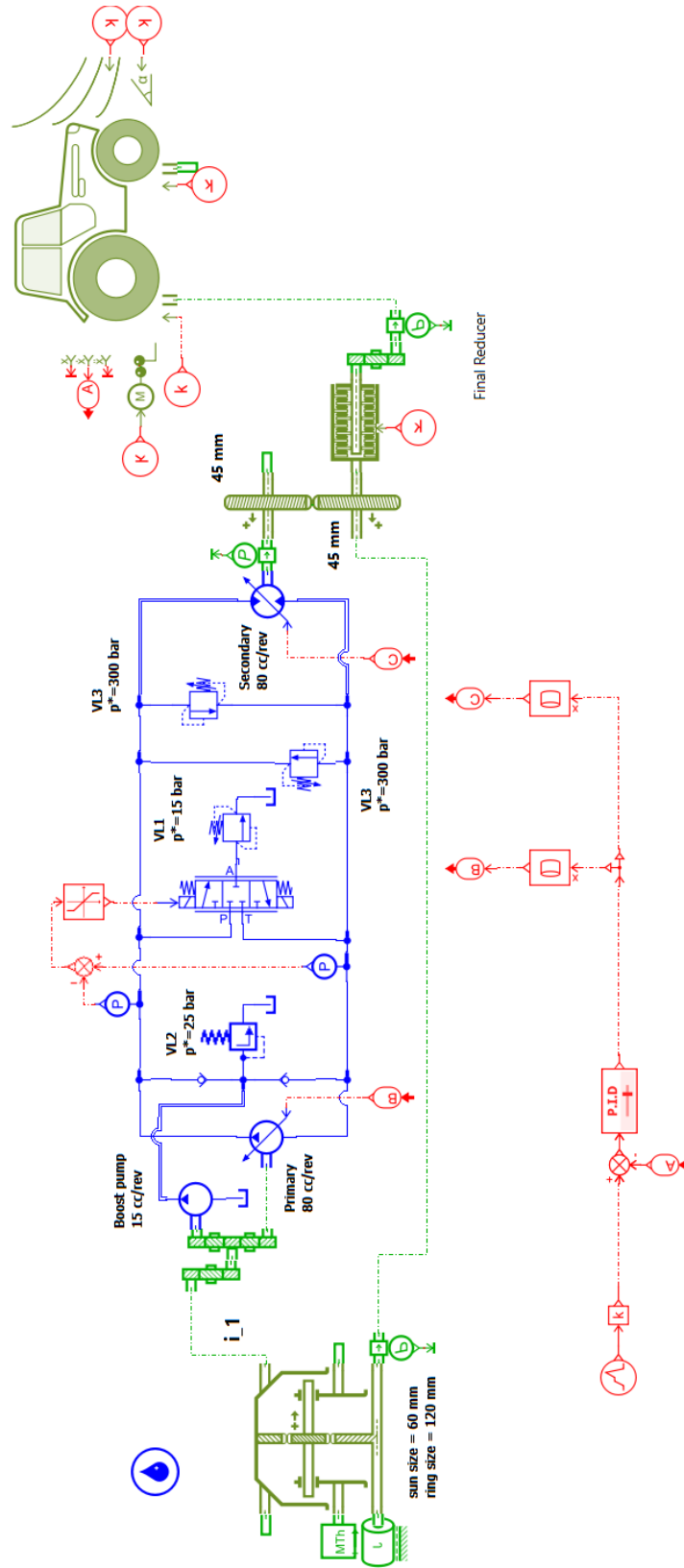
Simulations on inclined surfaces revealed how each configuration adapts to increased load. In particular, the IC configuration's higher planetary gear ratios ( $\tau_0$ ) enabled smoother transitions and a greater share of mechanical power at high speeds, which is advantageous for high-speed applications.

## Bibliography

- [1] A. Rossetti, A. M. (2011). Optimization of hydro-mechanical power split transmissions. *Elsevier*.
- [2] Blake Carl, M. I. (2006). Characteristics in Power Split Continuously Variable Transmissions evolution and future trends. *SAE*.
- [3] Carl, B., Ivantysynova, M., & Williams, K. (2006). Comparison of Operational Characteristics in Power Split . *SAE International*.
- [4] Jin Yu, Z. C. (2017). Hydro-mechanical power split transmissions: Progress evolution and future trends. *Sage*.
- [5] Kress, J. H. (1968). Hydrostatic Power-Splitting Transmissions for Wheeled Vehicles — Classification and Theory of Operation. *SAE International*. Retrieved 3 15, 2024, from <https://sae.org/publications/technical-papers/content/680549>
- [6] Naunheimer, H. B. (2011). *Automotive Transmissions*. Springer.
- [7] Scamperle, M. (n.d.). *Advanced Design Methods For Hydromechanical Transmissions In Road And Agricultural Vehicles*. University of Padua.
- [8] Vacca, A., & Franzoni, G. (2021). *Hydraulic Fluid Power: Fundamentals, Applications, and Circuit Design*. John Wiley & Sons.

# Appendix

## Output Coupled HMT plant using PID control



# Input Coupled HMT plant using PID control

